

---

Dr. Josep M<sup>a</sup> Chimenos Ribera

*Departament de Ciència de Materials i  
Química Física*

*Secció Departamental de Ciència i  
Enginyeria de Materials*



# Treball Final de Grau

**Characterisation of Weathered Bottom Ash for the critical metals recovery.**

**Caracterització d'Escograva per a la recuperació de metalls crítics.**

Susanna Pérez Martínez

*January 2018*



UNIVERSITAT DE  
BARCELONA

**B:KC** Barcelona  
Knowledge  
Campus  
Campus d'Excel·lència Internacional



Aquesta obra esta subjecta a la llicència de:

Reconeixement–NoComercial–SenseObraDerivada



<http://creativecommons.org/licenses/by-nc-nd/3.0/es/>



*Environmental pollution is an incurable disease. It can only be prevented.*

Barry Commoner

M'agradaria agrair el suport i l'ajuda que he rebut per part del meu tutor, el Dr. Josep M<sup>a</sup> Chimenos, i de tots els que han estat companys de laboratori al llarg de la meva estada al grup de recerca DIOPMA. Especial agraïment, entre ells, a la Dra. Jessica Giró per tots els seus consells i per ajudar-me sempre que ho he necessitat, i a l'Alex Maldonado per donar-me un cop de mà amb una de les parts més feixugues de l'experimental.

A més, una part dels coneixements que he adquirit al llarg de l'elaboració d'aquest projecte la deo al personal dels CCIUB, en Paco, la Maite, la Bárbara, l'Elisenda i la Maria, amb els quals he compartit moltes hores i s'han convertit en el meu "segon grup de recerca". També vull remarcar l'ajuda desinteressada de l'Ignasi Queralt, de l'IDAEA-CSIC, i l'interès que va mostrar en el meu treball.

Gràcies també a l'empresa VECSA, per deixar-me visitar les seves instal·lacions i proporcionar-me mostra i alguna informació que m'ha sigut de molta utilitat.

Finalment, i no menys important, dono les gràcies als meus familiars més propers, que han viscut l'evolució del projecte amb mi i m'han vist créixer al llarg de tot el grau de Química. I a tu, Zeno, per ser sempre al meu costat i per ajudar-me treure el millor de mi.



**REPORT**





# CONTENTS

<b>1. SUMMARY</b>	<b>3</b>
<b>2. RESUM</b>	<b>5</b>
<b>3. INTRODUCTION</b>	<b>7</b>
<b>3.1. Critical Metals</b>	<b>7</b>
<b>3.2. Bottom Ash Valorisation</b>	<b>8</b>
3.2.1. Metals in Bottom Ash	9
3.2.2. Weathered Bottom Ash	10
3.2.3. Importance of Weathered Bottom Ash's Characterisation	11
<b>3.3. Determination of Critical Metals in Weathered Bottom Ash</b>	<b>11</b>
3.3.1. Total Acid Digestion	11
3.3.2. Sequential Extraction	12
<b>4. OBJECTIVES</b>	<b>14</b>
<b>5. EXPERIMENTAL SECTION</b>	<b>15</b>
<b>5.1. Sample Collection</b>	<b>15</b>
<b>5.2. Previous Preparation of Weathered Bottom Ash</b>	<b>15</b>
5.2.1. Drying	16
5.2.2. Sample Division and Particle-Size Distribution by Sieves	16
5.2.3. Crushing and Milling	17
5.2.4. Metals Removal	18
<b>5.3. Characterisation of Weathered Bottom Ash</b>	<b>19</b>
5.3.1. IR Spectroscopy	19
<b>5.4. Analysis for the Metals Recovery Assessment</b>	<b>19</b>
5.4.1. Total Acid Digestion	19
5.4.2. Sequential Extraction	20
5.4.3. X-Ray Diffraction	22
5.4.4. X-Ray Fluorescence	23

<b>6. RESULTS AND DISCUSSION</b>	24
<b>6.1. Drying</b>	24
<b>6.2. Particle Size Distribution</b>	24
<b>6.3. Metals Removal</b>	25
<b>6.4. IR Spectroscopy</b>	25
<b>6.5. X-Ray Fluorescence</b>	26
<b>6.6. Analysis for the Metals Recovery Assessment</b>	27
6.6.1. Total Acid Digestion	27
6.6.2. Sequential Extraction	32
6.6.3. X-Ray Diffraction	36
<b>7. CONCLUSIONS</b>	37
<b>8. REFERENCES AND NOTES</b>	39
<b>9. ACRONYMS</b>	40
<b>APPENDICES</b>	41
Appendix 1: Particle Size Distribution Data	43
Appendix 2: Metals Removal Data	43
Appendix 3: IR Spectra for WBA	44
Appendix 4: XRF Results for WBA	45
Appendix 5: Total Acid Digestion Results	45
Appendix 6: Sequential Extraction Data	47
Appendix 7: XRD Results for WBA and for the Sequential Extraction Procedure	50

## 1. SUMMARY

Currently, modern high-technology industries have increased the use of precious metals and rare earth elements in Electric and Electronic Devices (EED). However, their natural resources are limited and have been exploited over the 60%, for most of them. Moreover, the economic or social situation of some metals providing countries supposes a high risk for their supply. The metals in this situation are called *critical metals*, and they are the main interest in the present project.

As the demand of critical metals is increasing due to the development of electronic industry, it is hugely important the search of sustainable and new sources. Incinerated municipal waste is a potential source of critical metals since a lot of EED are not recycled properly and incineration is a wide extended waste treatment in Europe. Weathered Bottom Ash (WBA) is the major by-product of incinerated municipal waste; therefore, it is the material used in this project to evaluate the valorisation of some selected critical metals contained.

A previous characterisation of WBA is carried out using different methods, such as particle size distribution, IR spectroscopy, X-ray fluorescence, and X-ray diffraction. The determination of the total amount of critical metals in WBA is performed by a total acid digestion. Besides, a sequential extraction is conducted to define their chemical form. Moreover, a comparison between WBA from two different seasons, winter and summer, is performed.

Results show that summer WBA sample contains more metals than winter WBA sample. The main metals in both samples are Al, Mg, and Cu, whereas the minor metals founded are Au, Ge, In, Ir and Ta. Furthermore, most of the critical metals evaluated are founded in the last step of the sequential extraction (residual), which means that they are in their crystalline structure and well stabilised in the matrix of the material, thus they cannot be extracted easily.

**Keywords:** Weathered bottom ash, critical metals, sequential extraction, total acid digestion, valorisation.



## 2. RESUM

Actualment, la indústria de l'alta tecnologia modera ha augmentat considerablement l'ús de metalls preciosos i elements de terres rares per la fabricació de dispositius elèctrics i electrònics. Tanmateix, les fonts naturals d'aquests metalls són limitades i, per la majoria d'ells, ja s'han explotat per sobre del 60%. A més a més, la situació econòmica i social d'alguns països proveïdors de metalls suposa un alt risc per al seu subministrament. Els metalls en aquesta situació s'anomenen *metalls crítics* i són el principal interès del present projecte.

Donat que la demanda de metalls crítics va en augment degut al desenvolupament de la indústria de l'electrònica, és de gran importància la recerca de fonts noves i sostenibles. Els residus municipals incinerats són una font potencial de metalls crítics, ja que una gran quantitat de dispositius elèctrics i electrònics no són reciclats adequadament i la incineració és una tècnica de tractament de residus molt estesa arreu d'Europa. L'Escograva és el subproducte majoritari de la incineració de residus municipals i; per tant, és el material d'estudi d'aquest projecte per l'avaluació de la valorització dels metalls crítics que conté.

Inicialment es du a terme una caracterització de l'Escograva utilitzant diferents mètodes, com la distribució de mida de partícula, l'espectroscòpia IR, la fluorescència de rajos-X i la difracció de rajos-X. La determinació del contingut total de metalls crítics a l'Escograva es realitza per mitjà d'una digestió àcida total, així com també es du a terme una extracció seqüencial per tal de definir-ne l'especiació química. A més a més, s'estableix una comparació entre Escograva de dues estacions de l'any diferents, hivern i estiu.

Els resultats mostren que l'Escograva de l'estiu conté una major quantitat de metalls crítics que la de l'hivern. Els metalls majoritaris trobats a ambdues mostres són Al, Mg i Cu, mentre que els minoritaris són Au, Ge, In, Ir i Ta. Per altra banda, la majoria dels metalls crítics avaluats s'extreuen a l'última etapa de l'extracció seqüencial (residual), fet que significa que es troben ben estabilitzats en forma d'estructura cristal·lina i que no es poden extreure fàcilment.

**Paraules clau:** Escograva, metalls crítics, extracció seqüencial, digestió àcida total, valorització.



### 3. INTRODUCTION

Nowadays, the whole world depends on raw materials. The incoming of the industrial revolution in the middle of the 18<sup>th</sup> century changed completely the humanity and caused the begging of a period based on the consumption and massive exploitation of natural resources to produce goods and energy.

Dependence on non-renewable resources has increased exponentially to the point of being necessary the search of alternatives materials and renewable energy sources, so that the current first world level of comfort could be maintained. Nowadays the dependence on non-renewable materials has risen up to 96 % by weight [1].

#### 3.1. CRITICAL METALS

Metals are one of the most currently used non-renewable materials. Moreover, in the last century, the number of different used metals in the production of objects and devices has increased. For example, original telephones were made of metals such as chromium, iron, copper, zinc, tin, lead, and aluminium; whereas modern mobile phones can be made of many more different metals such as lithium, beryllium, yttrium, iridium, gold, silver, gallium, antimony, barium, thallium, dysprosium, and neodymium, as well as the previous mentioned. In consequence of that fact, some metals have already been mined up more than 60% of its total reserves in the earth's crust.

According to the European Commission, some metals present a higher risk of the shortage of supply (due to high import dependence and high level of concentration in few countries, sometimes politically or economically unstable) and a big importance for the economy of specific sectors. Moreover, there is a lack of substitutes for a lot of these metals [2]. The metals in this situation are called **critical metals** and they are the aim of the study of the present project.

The critical metals considered by the EU in 2017 are as follows: antimony, barium, beryllium, bismuth, cobalt, gallium, germanium, hafnium, indium, iridium, niobium, palladium, platinum, rhodium, ruthenium, tantalum, tungsten, vanadium and some rare earth elements [3].

Most of the critical metals are in very low quantities in most of new technology devices and are increasingly essential to the development of sustainable and smart production, extremely related to energy efficiency and environmental technologies.

Due to the difficulty to mine these critical metals and to research for alternatives, it is important to recycle the objects which contain them. However, our society has not received enough knowledge about this need and has real problems to throw them out in the correct place for its recycling at the end of their useful life. That is why a large amount of Electric and Electronic Devices (EED) are thrown away every year in the refuse trash bins of Municipal Waste (MW), making almost impossible to recuperate those valuable metals contained. This type of waste is often called WEED (Waste of Electric and Electronic Devices) or E-waste.



**Figure 1.** The E-waste centre of Agbogbloshie, in Ghana, where electronic waste is burnt and disassembled without safety and environmental consideration. (Source: Marlene Napoli - Own work, CC0, 18/11/17 via Wikimedia Commons, Creative Commons Attribution)

### 3.2. BOTTOM ASH VALORISATION

Incineration is the main treatment of Municipal Waste (MW) in Europe and its technology is developing rapidly all around the world. It allows the reduction of the 20 % of the initial volume and the reduction of mass up to the 80-90 %: for each incoming tone of MW to the incineration plant, about 180-250 kg of Bottom Ash (BA) is produced [4]. BA is the major by-product of MW incineration plants, which is catalogued as a non-hazardous material [5], and it is usually reused as a raw recycled material in substitution for natural sand and gravel. It is mainly composed of silicon, calcium, iron, aluminium, and sodium. However, it also contains a considerable amount of heavy metals and, therefore, in some countries is managed in landfills [6].



In Catalonia, the current legislation allows the valorisation of BA after its removal of ferrous metals, which is usually carried out using magnets. Then, BA can be used as road-base aggregate, levelling of embankments and land, provisional ways, filler for the restoration of degraded areas, and other activities authorized by the *Junta de Residus* of Catalonia. However, BA is forbidden to be used in flooding areas, nearer than 30 m of a river or a torrent, in areas with the phreatic zone nearer than 5 m, more proximal than 100 m of an exploitation of groundwater, and in areas where the material of the soil is fragile [7].



**Figure 2.** Bottom ash before valorisation. (Image extracted from the website *VECSA. Instalaciones*. Downloaded on 12/11/17 from <http://www.vecsa.es/la-empresa/instalaciones>)

### 3.2.1. Metals in Bottom Ash

During the incineration process of MW, metals behaviour depends on their willingness to react and change form. Mercury and cadmium are examples of volatile metals that can be lost during incineration and can be considered negligible in BA. Other non-volatile metals can suffer different behaviour when incinerated. Metals with low melting point as Al or Zn (660.32 °C and 419.53 °C, respectively [8]) will melt and afterwards solidify when the temperature drops down. Other metals with higher density, such as Cu, Au, Ag, and Sn, have no significant damage or oxidation. Therefore, these metals will remain in their original metallic form during incineration, hence will have recycling value.

Separation of metallic particles has two main benefits: a) allowing its recycling and b) improvement of the material's mechanical properties, thus it can be reused in a wide range of construction purposes [4].

### 3.2.2. Weathered Bottom Ash

In the incineration plant of SIRUSA, located in Tarragona, the BA produced is carried to VECSA's facilities, a company that performs its conditioning and valorisation.



**Figure 3.** Installations of VECSA. (Image extracted from the website *VECSA. Instalaciones*. Downloaded on 12/11/17 from <http://www.vecsa.es/la-empresa/instalaciones>)

The first stage of the process is the separation of particles bigger than 30 mm from the rest of the material. Both two resultant parts are then subjected to different treatments with the aim of removing ferrous and non-ferrous metals and lightweight particles, such as plastics, papers or clothes, and obtaining a homogenized granular material. After these conditioning processes, the bigger material is crushed to reduce its particle size and is joined to the smaller part of the BA. Finally, another treatment is carried out to remove remaining ferrous particles. Metals extracted from BA are classified for its reuse. The BA after this process is stored in contact with air and tossed periodically during two to three months, in which time it is chemically stabilized for its commercialization under the name Weathered Bottom Ash (WBA) or *Escograva* in Catalan [9]. This last step, called *natural weathering*, is as simple as important to assure the use of WBA since its reactivity and the leaching of metals is considerably reduced. This results from [4]:

- Carbonation due to the uptake of  $\text{CO}_2$ , and consequentially lower pH to 8-10.
- Hydration of the mineral phases.
- Sorption of dissolved heavy metals in the matrix of the material.
- Changing binding characteristics of available ligands.
- Leaching of highly dissolved salts.

### 3.2.3. Importance of Weathered Bottom Ash's Characterisation

As WBA is mainly used in construction as road-base aggregates, embankments, provisional ways, or construction filler, among others, it is very significant to determine its composition and to establish and guarantee its safety for human health and environment.

Although ferrous and non-ferrous metals have been removed from BA in the process to obtain WBA, these process is effective for the particle size fraction higher than 8–10 mm. Therefore, it is well known that there are some remaining metallic particles in it, mainly in the fine fractions, mostly coming from the EED waste and other metallic devices contained[10]. Those metals might be potentially released to the environment through the rain or the erosion made by other environmental factors. In this sense, water leaching test is usually used to determine the potential of the heavy metals release.

Moreover, the characterisation of WBA can be useful to evaluate the recovery of metals contained. It is important to emphasise that the viability of metals recovery strongly depends on its chemical form and its ability to release under different treatments. The characterisation can be carried out through different methods. Section 3.3 contains a description of the characterisation methods used.

## 3.3. DETERMINATION OF CRITICAL METALS IN WEATHERED BOTTOM ASH

### 3.3.1. Total Acid Digestion

Total acid digestion a widely used method to quantify the total amount of each element contained in a solid sample. It consists, in general, of a multiple-step digestion applying different strong mineral acids and heat, until the complete solution of the analytes and the complete decomposition of the solid matrix. Other liquid reagents, such as  $H_2O_2$ , can also be used. Finally, the dissolved sample is analysed by Inductively Coupled Plasma, Atomic Absorbance Spectrophotometry (AAS) or Atomic Fluorescence Spectrometry (AFS), as examples.

The selected reagents depend on the mineral phases and nature of the sample to be digested. It is highly important to considerer the solubility of the resulting salts of the present

metals after the digestion in order that the solution remains stable. These are the effects of each reagent used on some metals [11]:

- **Nitric acid:** forms soluble nitrates with all the elements except Au, Pt, Al, B, Cr, Ti and Zr.
- **Nitric acid and hydrogen peroxide:** increase oxidation potential.
- **Hydrofluoric acid:** decomposes silicates.
- **Hydrochloric acid:** forms soluble chlorides with all elements except Ag, Hg, Ti; dissolves salts of weaker acids; digests iron alloys; oxides of Al, Be, Cr, Sb, Sn, Si, Ti and Zr are insoluble.
- **Perchloric acid:** decomposes organic matter when hot and concentrated [12].

### 3.3.2. Sequential Extraction

Sequential extraction is a procedure that allows separating the metals in a sample depending on their chemical forms. This study can be complementary to a total acid digestion since not only it gives the quantitative content of each element but also the chemical speciation of the analysed elements. The principle of the sequential extraction is the treatment of the solid sample in several consecutive steps with different solutions of increasing intensity of aggression. Each step leads to a solution separated by centrifugation, and a residual solid, which is then subjected to the next extraction solution.

The most common procedure for the sequential extraction was set up by A. Tessier in 1979, which is based on five fractions [13]:

1. **Ion exchange fraction:** metals absorbed on the surface of solid particles can pass to the solution easily.
2. **Carbonate fraction:** metals bound to carbonates are released to the solution.
3. **Iron and manganese oxides fraction:** metals bound to iron and manganese oxides are sensitive to changes in redox potential and metals can migrate to the solution under reducible conditions.
4. **Organic matter fraction:** trace metals that are bound to different types of organic matter can be released under oxidizing conditions.

5. **Residual fraction:** the residue of the last four steps contains mainly mineral metals in their crystalline structure. They can only be released under strong acid treatment.

Nevertheless, there are other procedures of sequential extraction developed recently. The one carried out in the present project is the BCR procedure, developed by the Community Bureau of Reference within the Standard Measurement and Testing Programme, which differs from the Tessier procedure in the number of steps and reagents used. This procedure has been widely used in samples of dust and ash. The steps are described as follows [6]:

1. **Ion exchange and carbonate fraction:** metals present in their ionic form on the surface of solid particles and bound to carbonates are released to the solution.
2. **Hydroxide fraction:** metals bound to iron and manganese oxides are sensitive to changes in redox potential and metals can migrate to the solution under reducible conditions.
3. **Organic matter fraction:** trace metals that are bound to different types of organic matter can be released under oxidising conditions.

A fourth step of a **Residual fraction** can be added to the process to complete it, although it is not present in the original BCR procedure.

## 4. OBJECTIVES

The main objective of the present project is to evaluate the possibility of recovering the critical metals from the municipal solid waste incineration bottom ash, depending on their content and chemical speciation, which allows evaluating the economic and technological viability.

However, in order to achieve the main objective, other specific objectives are derived, such as:

- Characterisation of WBA from a MW incineration plant, using different techniques specific for granular material characterisation.
- Determination of the total content of critical metals in WBA using a total acid digestion.
- Determination of the total content of critical metals in WBA and its chemical form using a modified BCR procedure of sequential extraction.
- Comparison between the quantitative results of the total acid digestion and the sequential extraction performed.
- Comparison between the total content of metals in two samples of bottom ash collected in February and July 2017, using a total acid digestion, with the aim to see any differences in waste from different seasons.

## 5. EXPERIMENTAL SECTION

The present project is based on the study of two samples of WBA collected on different months, which represent different seasons: winter and summer, both collected before starting this project.

This section covers the experimental procedures performed in WBA samples and the techniques used for the samples' preparation and characterisation. Moreover, a brief description of the instrumental parameters used in the different processes is also included.

### 5.1. SAMPLE COLLECTION

WBA from the VECSA facilities (Tarragona) has been picked up on the last February and July.

It is well known that WBA is highly heterogeneous, as it contains different types of ceramics and metals, and a low percentage (<5 %) of flammable materials (e.g. plastics, paper, etc...) and organic matter [10]. Hence, it is needed to take WBA from different arbitrary parts of the whole pile (*Figure 2*). Around 33 kg of February WBA and 17 kg of July WBA were collected by using plastic spades, and the samples were stored in a 30 L plastic container.

### 5.2. PREVIOUS PREPARATION OF WEATHERED BOTTOM ASH

The preparation of WBA has been performed in DIOPMA research group laboratories and in the Scientific and Technological Centers of the University of Barcelona (CCiTUB), in the *Servei de Làmina Prima* from the Geology Faculty at the University of Barcelona. The following scheme (*Figure 4*) shows the procedure of the samples' preparation, described in the following sections.

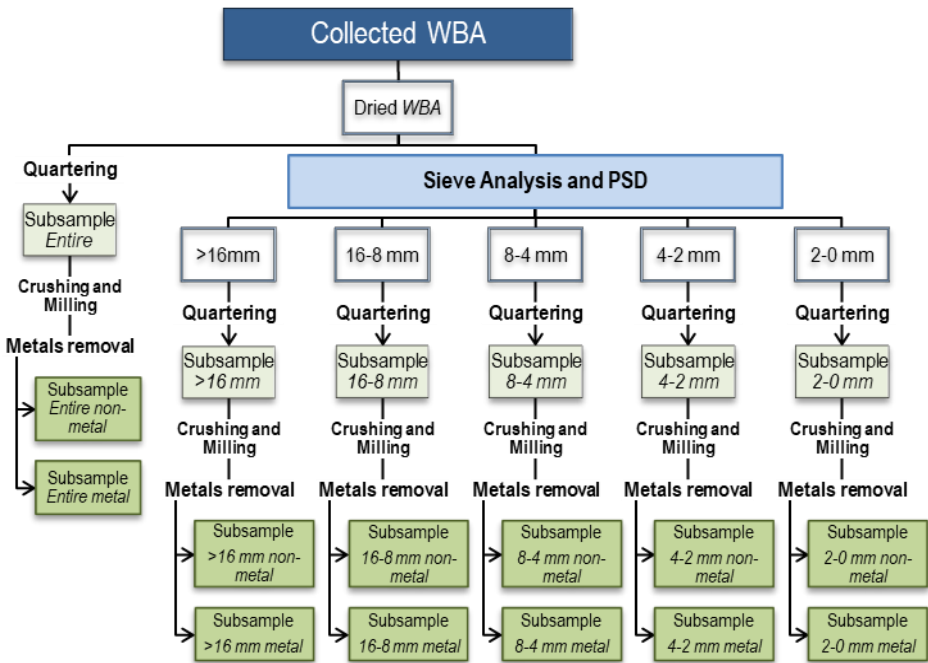


Figure 4. Simplified scheme of the preparation of the samples.

### 5.2.1. Drying

Previous to the characterisation or treatment of the sample, a drying process is required. Drying is carried out using a heater P SELECTA, model *Conterm*, at 105 °C during 24 h. The percentage of moisture is calculated for both WBA samples (February and July). The following Equation 1 is considered:

$$\% \text{ Moisture} = \frac{WM - DM}{DM} \cdot 100 \quad (\text{Equation 1})$$

**Equation 1:** Moisture calculus for a solid. WM is the *Wet Mass* and DM is the *Dry Mass* of the solid.

### 5.2.2 Sample Division and Particle-Size Distribution by Sieves

Particle Size Distribution (PSD) of a sample consists of the determination of the amount of matter (usually by mass) which can be classified depending on its particle size. Sieve analysis is the most common way to determine the PSD, which consists of the usage of sieves to separate the sample into different subsamples, each between two particle sizes.



For the characterisation of WBA, it is interesting to divide it into five fractions of different particle size, in addition to the 'entire sample' as it is. The aim of this division is to have more accurate results and to be able to compare the amount of metals in each fraction of the sample and to determine if there is a higher concentration in one specific particle size fraction. Thus, the resulting six fractions are (as mentioned above, in *Figure 4*): Entire, >16 mm, 16-8 mm, 8-4 mm, 4-2 mm and 2-0 mm.

However, before separating the sample according to different particle size, the subsample Entire must be obtained by reducing the size of the initial sample (1/16) into a representative part of 50-100 g, first using a riffle splitter and then quartering manually when the amount is smaller enough. Particular attention must be paid to avoidance of loss of fines during this operation.

Then, the rest of the whole sample is sieved to separate it according to the other five fractions, using a sieve shaker RETSCH, model AS200, and its corresponding set of sieves, as shown in *Figure 5*. The weight of each particle size fraction obtained is used to determine the PSD of WBA. Comparison between PSD of WBA from February and July has been represented in *Figure 10*, section 6.2. When the five fractions are separated, each one is quartered (1/16) to obtain subsamples of 50-100 g, as presented in *Figure 6*.



**Figure 5.** Sieve shaker RETSCH AS200, while working.



**Figure 6.** Subsamples according to the PSD, obtained after quartering 1/16 (from left to right and from top to bottom: Entire, >16 mm, 16-8 mm, 8-4 mm, 4-2 mm and 2-0 mm).

### 5.2.3 Crushing and Milling

Both crushing and milling operations have been carried out in the CCiTUB facilities of the *Servei de Làmina Prima* of the Faculty of Geology of University of Barcelona. All the

subsamples have been firstly crushed in a jaw crusher RETSCH model *BB51*, and subsequently milled in a vibratory disc mill RETSCH, model *RS100*, using a grinding set made of hardened steel. Milling is applied until the whole sample passes through a sieve of 80  $\mu\text{m}$  mesh.

### 5.2.4 Metals Removal

It is interesting to remove the metal particles from the six samples milled for some reasons: first, the amount of metal particles is a minority compared to the total mass of the sample, and separating them to form a new subsample is a way to obtain more precise results; also because, for some techniques such as X-ray diffraction or X-ray fluorescence, the presence of metallic particles can be a problem for the preparation of samples for their characterisation.

With this aim, non-magnetic metal particles in the subsamples have been collected sieving the milled samples. A sieve of 750  $\mu\text{m}$  mesh was fitted on the sieve of 80  $\mu\text{m}$  with the aim to retain those big metal particles which have been deformed during the milling instead of fractioned, due to their ductile property. Moreover, magnetic metal particles have been removed passing a magnet (Nd; 0,485 T) over the sample, wrapped in a little plastic zip bag. This operation might have been done more than once to ensure most of those particles are removed.

All the metallic matter is kept separately. Hence, up to now, the subsamples are divided into 'metal' and 'non-metal' subsamples. Altogether there are 12 subsamples to be characterised and analysed: **Entire metal**, *Entire non-metal*, **>16 mm metal**, *>16 mm non-metal*, **16-8 mm metal**, *16-8 mm non-metal*, **8-4 mm metal**, *8-4 mm non-metal*, **4-2 mm metal**, *4-2 mm non-metal*, **2-0 mm metal** and *2-0 mm non-metal*.

The previously mentioned process has been applied to WBA from both February and July since these are the samples which are going to be compared after an acid digestion.



**Figure 7.** Final 12 subsamples from July prepared for their characterisation and analysis (on the top from left to right: Entire non-metal, >16 mm non-metal, 16-8 mm non-metal, 8-4 mm non-metal, 4-2 mm non-metal and 2-0 mm non-metal; on the bottom: the corresponding metal sample of samples above them).

### 5.3. CHARACTERISATION OF WEATHERED BOTTOM ASH

Preparation and characterisation of the sample is needed before carrying out any analytical procedure. IR spectroscopy, X-Ray Diffraction (XRD) and X-Ray Fluorescence (XRF) are some typical characterisation techniques for powder samples which have been used. IR spectroscopy is described in the following section (5.3.1), whereas analysis of XRD and XRF, are described in sections 5.4.3. and 5.4.4.

#### 5.3.1. IR Spectroscopy

IR spectroscopy has been applied to characterise all non-metal subsamples from July and the *Entire non-metal* subsample from February, with the aim to see any differences between subsamples of different particle size and to compare samples between two different months. The FT-IR device used in this project was a Spectrum Two™ from Perking Elmer supported by Dynascan™ interferometre and OpticsGuard™ technology. This equipment can measure substances at liquid and solid state, it is optimized by a wavelength range between 4000 cm<sup>-1</sup> and 350 cm<sup>-1</sup> (mid-IR segment) and its standard spectral resolution is 0.5 cm<sup>-1</sup>. Samples must be completely dried and milled under 80 µm of particle size to obtain comparable results. IR spectra have been obtained and interpreted with adequate software. Characteristic peaks for each sample have been classified and assigned.

### 5.4. ANALYSIS FOR THE METALS RECOVERY ASSESSMENT

#### 5.4.1. Total Acid Digestion

Total acid digestion of the 12 subsamples from February and July has been carried out to quantify those critical metals studied. The procedure has been done in the Laboratory for Metals Analysis of the CCiTUB. The experimental procedure carried out is as follows:

0.1 g of sample, previously milled and homogenized, is weighed in Teflon reactors. Besides, 2.5 mL of concentrated HNO<sub>3</sub> is added and the reactor is closed and left overnight in an oven at 90 °C. Subsequently, the content in the reactors is transferred to centrifuge tubes and centrifuged. The floating liquid is taken with a pipette and both the remaining solid and the reactor are washed with ultrapure water and centrifuged until necessary. Floating liquid of each

centrifugation is transferred to a 100 mL volumetric flask and those are filled up with ultrapure water. The residue from centrifugation is moved again to the Teflon reactors adding 5 mL of HF, 2.5 mL of HNO<sub>3</sub> and 2.5 mL of HClO<sub>4</sub>, all acids concentrated. Reactors are left overnight in an oven at 90 °C. Later, the content in the reactors is transferred to Teflon vessels and heated in a sand bath until white smoke appears, which indicates that both HNO<sub>3</sub> and HF have evaporated and HClO<sub>4</sub> is evaporating. In this moment, an oxidising treatment should be applied adding 2.5 mL of concentrated HNO<sub>3</sub> and 2.5 mL of H<sub>2</sub>O<sub>2</sub> at 30%, and leaving in reflux for a while. After that, samples are heated again in a sand bath until seeing white smoke. Oxidising treatment must be repeated two more times. Finally, samples are left in the sand bath until it only remains approx. 1 mL of HClO<sub>4</sub> in the vessels; then, it is redissolved in 2 mL of *aqua regia* (0.5 mL HNO<sub>3</sub> and 1.5 mL HCl, concentrated) and 5 mL of ultrapure water, transferred to 100 mL volumetric flask and filled up with ultrapure water.

Leachates obtained are analysed using Inductively Coupled Plasma Mass Spectrometry (ICP-MS) and Inductively Coupled Plasma Optical Emission Spectrometry (ICP-OES) at CCiTUB. The metals quantified are the following: Ag, Al, Au, Be, Co, Cu, Ga, Ge, In, Ir, Li, Mg, Ni, Pd, Pt, Sb, Ta, and W. Additionally, two blanks should be carried through the complete procedure and analysed at the end together with the other samples.

The list of metals analysed differs from those critical metals established by the European Community for some reasons: on the one hand, the amount of some critical metals, as rare earth ones, would be in extremely low concentrations in WBA (such as rhodium and ruthenium [14]) and the limit of detection for ICP-MS technique will not allow to determine them correctly; on the other hand, there are metals which are not considered critical but are interesting to be recovered because of their abundance in the sample showed in previous studies ([14], [15]), these are Al, Li, Mg and Ni. Also, other metals are added, Ag and Au, because of their high market price.

#### 5.4.2. Sequential Extraction

Sequential extraction for the 12 subsamples from July has been performed to determine the chemical speciation of the critical metals contained, which will define the ease of those metals to be released to the environment and, thus, the viability of critical metals recovery.

A modified BCR sequential extraction procedure is applied to the WBA samples, defined by G. Rauret *et. al.* in 1998 [16]. In this procedure, an extra step of total digestion with *aqua regia* is added by recommendation at the end of the original procedure. However, in the present project, the total digestion of the last residue has been done using other strong acids, following the procedure described in section 5.4.1. Moreover, another step with water as a reagent was added at the beginning of the procedure to simulate a leaching test, since the water is the most simple and available reagent if the recovery should be done in a large scale. The final procedure and the quantity of reagents used are:

1. **Exchangeable fraction:** 1 g of the sample is extracted by shaking for 16 h (overnight) at room temperature with 40 mL of ultrapure water.
2. **Carbonate fraction:** the residue from the previous step (residue 1) is extracted with 40 mL of acetic acid 0.1 M ( $\text{pH} \approx 2.9$ ), by shaking for 16 h (overnight).
3. **Hydroxide fraction:** the residue from the previous step (residue 2) is extracted with 40 mL of a solution of hydroxylamine hydrochloride 0.5 M acidified with 2.5 % of  $\text{HNO}_3$  2 M ( $\text{pH} \approx 1.3$ ), by shaking for 16 h (overnight).
4. **Organic matter fraction:** the residue from the previous step (residue 3) is extracted with 10 mL of hydrogen peroxide of 30 % adjusted to  $\text{pH}=2-3$  with  $\text{HNO}_3$ , by shaking for 1 h, covered and at room temperature. Later, the uncovered solution is shaken at  $85 \pm 2^\circ\text{C}$  in a water bath for an hour. Then, further 10 mL of hydrogen peroxide (30 %,  $\text{pH}=2-3$  with  $\text{HNO}_3$ ) are added and the covered sample is heated to  $85 \pm 2^\circ\text{C}$  in a water bath for an hour. Finally, the cover is removed, and the volume of liquid is reduced to 1 mL by heating. 50 mL of ammonium acetate 1 M are added, and the sample is extracted for 16 h (overnight) by shaking.
5. **Residual fraction:** the residue of the previous step (residue 4) is digested following the procedure described in the section 5.4.1. The leachates obtained are analysed using ICP-MS (Perkin Elmer Elan 6000) and ICP-OES (Perkin Elmer Optima 8300) at CCiTUB. The metals quantified are the same analysed for the total acid digestion: Ag, Al, Au, Be, Co, Cu, Ga, Ge, In, Ir, Li, Mg, Ni, Pd, Pt, Sb, Ta, and W.

Extractions have been performed in 100 mL centrifuge tubes made of HDPE, as shown in Figure 8. After each step, samples have been centrifuged (centrifuge MSE, model Pacisa) at 3000 rpm for 25 min. The liquid was separated using a manual pipette, filtered with a  $0.45\ \mu\text{m}$

pore filter and acidified with two drops of concentrated  $\text{HNO}_3$  for its analysis with ICP-MS and ICP-OES. Reagents have been prepared using analytical chemicals and ultrapure water (simple deionized water should not be used as it might contain some metal ions complexed to organic matter). In the case of hydroxylamine hydrochloride 0.5 M, the extractive solution should be prepared fresh the day it is needed.

Sequential extraction for the 12 subsamples obtained for WBA from July has been conducted in duplicated, thus the number of sequential extraction to be performed is 24. Moreover, 5 replicates of the Entire non-metal sample have been performed, with the aim to take off one residue in each step to characterise it. As the number of samples was too high to be performed simultaneously, four series of sequential extraction have been carried out, with a different blank for each of them. A blank for each series of sequential extraction have been carried through the complete procedure and analysed at the end of each extraction step, together with the other samples.



**Figure 8.** Assembly for the sequential extraction procedure.

### 5.4.3. X-Ray Diffraction

Powder XRD has been carried out to determine crystallinity (non-amorphous part) of the material (WBA) and which crystalline phases it does contains. Although a quantitative study can be done using XRD, it has been only used with a qualitative aim. *Entire non-metal* sample from the month of July and its replicate residues from the four steps of the sequential extraction have been analysed using XRD, to determine the degradation of the material in each step as well as the mineralogical changes in elements.

The equipment used is the one in the CCiTUB XRD service, which is a Panalytical equipment, model *X'Pert PRO MPD Alpha 1*. The sample preparation is simple and consists of making a powder amount back-loading in a special mould for Panalytical equipment. The sample must be completely dried and milled under 80  $\mu\text{m}$  of particle size. X-ray diffractograms have been obtained and qualitatively interpreted using *X'Pert HighScore* programme from Panalytical.

#### 5.4.4. X-Ray Fluorescence

XRF technique has been used in this project to quantify the amount of the main elements in the sample, expressed in percentage of their most stable oxides. Samples from February has been analysed in the CCiTUB XRF service, while samples from July have been analysed by Ignasi Queralt, from IDAEA-CSIC. For their XRF analysis, samples from February were prepared in fused glass disks using an induction furnace *Perle'x 3* from Panalytical. In this process, samples are dissolved and mixed into lithium tetraborate at a temperature around 1000 °C, in a platinum melting pot heated by induction. The sample is automatically poured into a pre-heated mould and cooled. Then, fused glass disks are analysed in a spectrophotometer Panalytical Philips PW 2400 sequential X-ray, equipped with the software UniQuant® V5.0. Before preparing the glass disks, the samples must be subjected to a heat treatment until 900 °C. On the other hand, samples from July are prepared for their XRF analysis by pelletizing, adding an additive to bind together and to harden the pellets. Samples are needed to be simply dried.

Due to problems in the samples' preparation process, the non-metal subsamples were the unique samples analysed by XRF. In the preparation of fused disks, metal particles do not achieve a complete fusion and the disks get broken when solidify; whereas in the preparation of pellets, metal particles would not allow to have a flat enough surface for an appropriate detection of elements. Results from both samples from different months are not compared, as the preparation of samples and the equipment have been different for each one. Moreover, only results for main metals are given, since minority metals are not detected properly.

XRF analysis has been carried out for the sequential extraction residues of the *Entire non-metal* subsample, as well. The purpose is to verify the loss of certain metals in each step of the extraction. Due to the little amount of solid available, these specific samples are analysed using the loose powders preparation technique, which consists of spreading out the material on a special film material "invisible" to X-Rays fixed attached to a cylindrical cup, as seen in *Figure 9*.



**Figure 9.** Cups for loose powders sample preparation, with the samples spread inside.

## 6. RESULTS AND DISCUSSION

### 6.1. DRYING

The result of the average moisture percentage obtained using *Equation 1*, after drying both samples from July and February, is  $13.7 \pm 0.4 \%$ .

### 6.2. Particle Size Distribution

PSD determined analysing the WBA samples from February and July is prepresented together for its comparison in *Figure 10*. Related data is presented in Appendix 1, *Table A.1*.

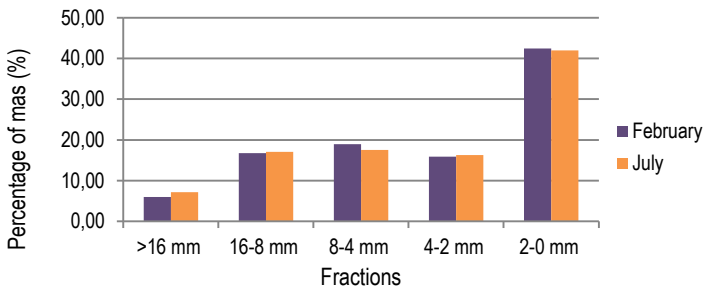


**Figure 10.** PSD for WBA from February and July.

As it is shown in the above *Figure 10*, WBA has a very constant PSD profile between seasons. The little differences are explained by the big heterogeneity of WBA; therefore, the collection of a representative homogeneous sample is very difficult to achieve.

Fraction 2-0 mm represents the main part of the total mass of the samples, as its percentage of mass is considerably higher than for the other fractions. On the other hand, fraction >16 mm is the less representative of the total sample. The most probable reason for that behaviour is that, during the process to obtain WBA from BA, particles bigger than 30 mm are crushed to reduce their size, and ferrous and non-ferrous metal particles are removed,



which are commonly the larger pieces. Moreover, smaller particles are the most abundant as they are produced during the process of incineration and crushing.

### 6.3. METALS REMOVAL

Fractions from February and July WBA, according to PSD, have been removed their metal particles using a magnet. The percentage for July WBA sample of metal and non-metal mass in each fraction is represented in *Figure 11*, whereas data for February WBA is attached in Appendix 2, *Table A.2*.

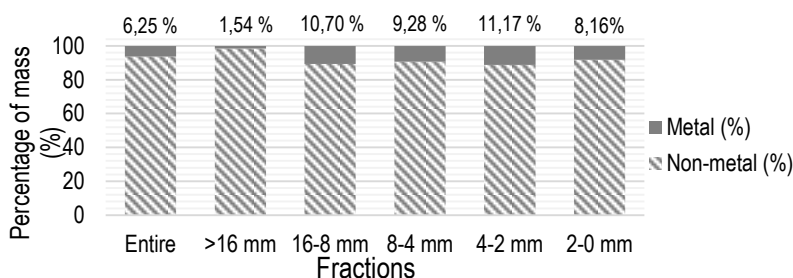


**Figure 11.** Percentage in mass of non-metal and metal part for July WBA.

There is no evident difference between the percentage of metal mass in all the fractions, except in the case of the fraction >16 mm, which has the lowest metal percentage (1.54 %). That fact may be explained again by the process to obtain WBA, since the ferrous and non-ferrous metals are extracted; therefore, the probability to have large pieces of metal in the sample of study is quite low.

### 6.4. IR SPECTROSCOPY

IR spectra have been obtained for all non-metal subsamples (Entire, >16 mm, 16-8 mm, 8-4 mm, 4-2 mm and 2-0 mm) of WBA from July and the Entire non-metal subsample of February.

All the spectra were compared, and they were very similar. Hence, it is not possible to establish significant differences between different particle size fractions using IR spectroscopy technique. IR spectra from the six particle size fractions of July WBA sample are overlapped and attached in *Figure A.1.* of Appendix 3 to verify their similarity. Besides, IR spectra for Entire fraction from July and February are overlapped in *Figure A.2.* of Appendix 3, as well. Peaks

have been identified for the sample Entire from July in *Figure 12*, and can be classified in general terms for the rest of the spectra, as is presented in *Table 1*.

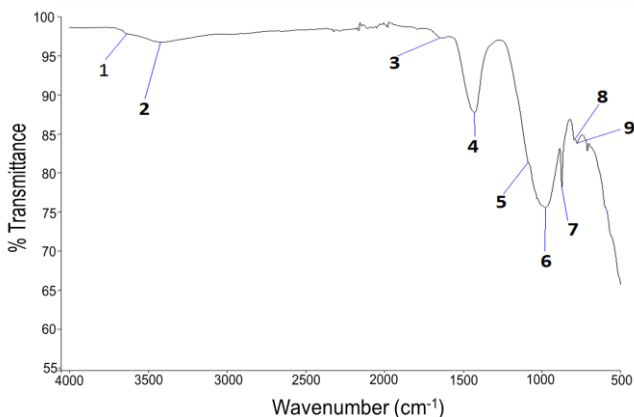


**Figure 12.** IR spectra for WBA from July, with its peaks identified.

**Table 1.** General assignments for IR frequencies obtained.

Number in Figure 12	Observed IR freq. [cm <sup>-1</sup> ]	Assignments
1	~3630	Stretching of O-H bond, resulting from Al(OH) <sub>3</sub> gels present [17]
2	~3400	Symmetric and asymmetric stretching for O-H of hydration water [17]
3	~1650	In-plane bending H-O-H of interlayer water [17]
4, 7	~1430 and ~870	Symmetric and asymmetric stretching for CO <sub>3</sub> <sup>2-</sup> , resulting from CaCO <sub>3</sub> present [17]
6	~980	Asymmetric stretching of Si-O bonds from quartz [18]
8, 9	~780-900	Symmetric stretching of the Al-O bond in aluminosilicate structure [18]

## 6.5. X-RAY FLUORESCENCE

Data obtained for non-metal fractions of February is presented in *Table A.3*. (Appendix 4), whereas XRF data for July WBA is also represented in *Figure 13*. It is remarkable that, for both samples, results show that the main elements of WBA are silicon, calcium, and aluminium, which coincide with the results for XRD analysis (section 6.6.3), where the clearest phases identified are made of these elements. Iron, magnesium, and sodium have enough concentration to be detected by XRF: iron is detected in XRD as well, whereas magnesium and sodium are not, which may confirm that exist mainly in amorphous phases. Manganese, titanium, and potassium are the less abundant main elements, and they are not detected in XRD.

Figure 13 shows the results for XRF analysis of July WBA, plotted depending on their particle size. As it can be seen, each element has a particular behaviour along the five particle size fractions; nevertheless, there are some elements with a similar conduct. This is the case of iron, calcium, and phosphorus, where the mass percentage of the element oxide decreases when decreasing the particle size. On the other hand, aluminium, magnesium, chlorine, calcium, sulphur, and titanium have a characteristic shape where central particle sizes have the minimum value. Sodium and silicon have the inverted shape, as the central particle sizes have the maximum value.

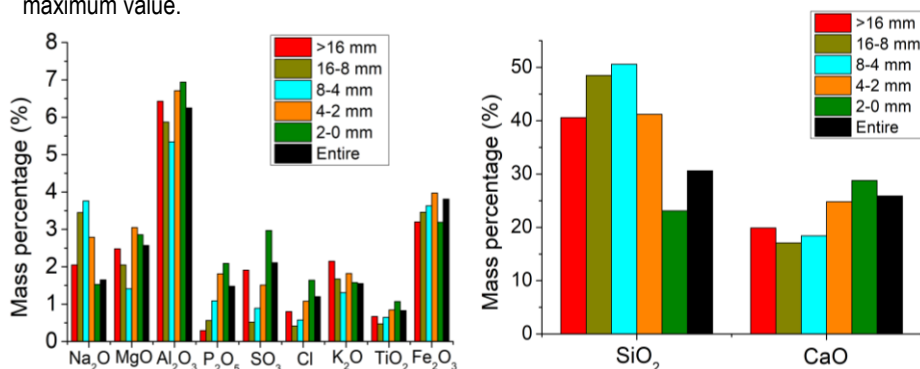


**Figure 13.** Mass percentage of the main elements given in their most stable oxides of July WBA, analysed with XRF technique and plotted according to the five particle size fractions.

Results of XRF analysis for the residues of the sequential extraction procedure (Appendix 4, Table A.4.) do not provide any clear conclusion since, for most elements, the concentration do not decrease from the initial sample to the residue of Step 4, as expected. Heterogeneity of the WBA can be an explanation for this fact, as each residue analysed comes from a different piece taken from the initial sample and a different replicate in the sequential extraction.

## 6.6. ANALYSIS FOR THE METALS RECOVERY ASSESSMENT

### 6.6.1. Total Acid Digestion

Acid digestion has given interesting results about the concentration (in  $\text{mg}\cdot\text{kg}^{-1}$ ) of the critical metals studied in the sample. Final results (content of metals in each particle size fraction and comparison with metal content in Entire fraction) should be calculated based on the ICP-MS results obtained for the 12 subsamples. The calculus is explained in Figure 14.

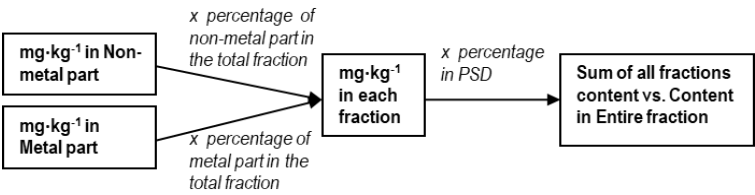


**Figure 14.** Scheme for the calculus of total acid digestion results.

A comparison has been established between the results for each fraction in February WBA and July WBA, shown in *Figures 15a* and *15b*. Tables with the related data are attached in *Table A.5.* and *Table A.6.* of Appendix 5.

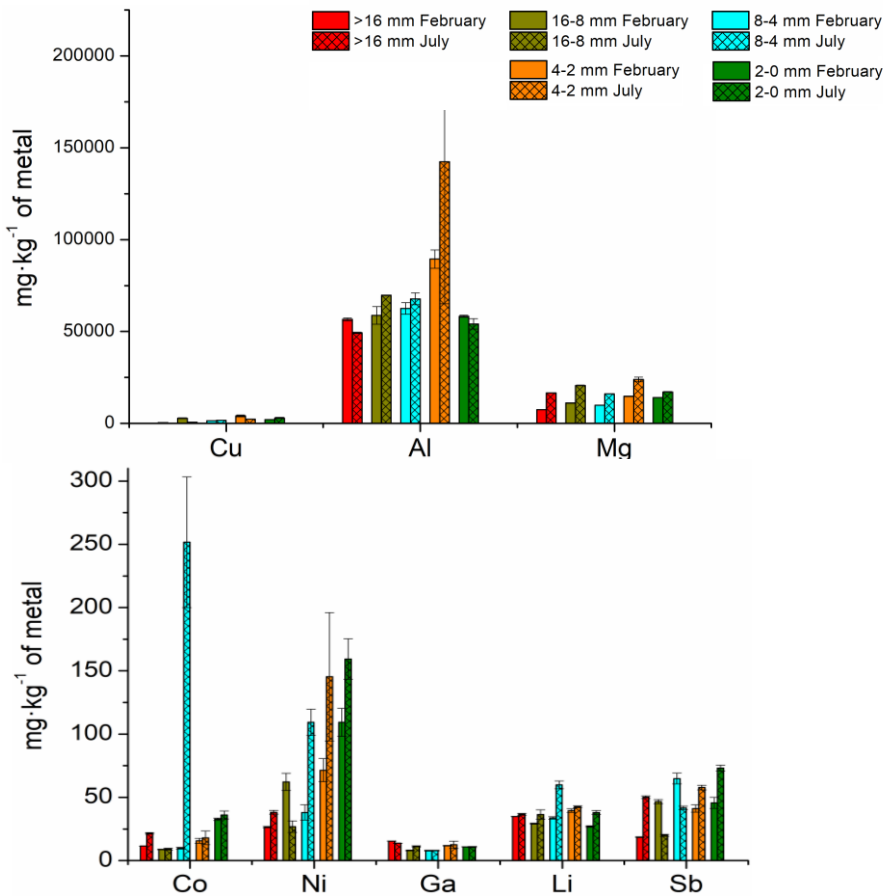


**Figure 15a.** Graphical comparison between the metal content in each particle size fraction for February WBA and July WBA, determined by total acid digestion.

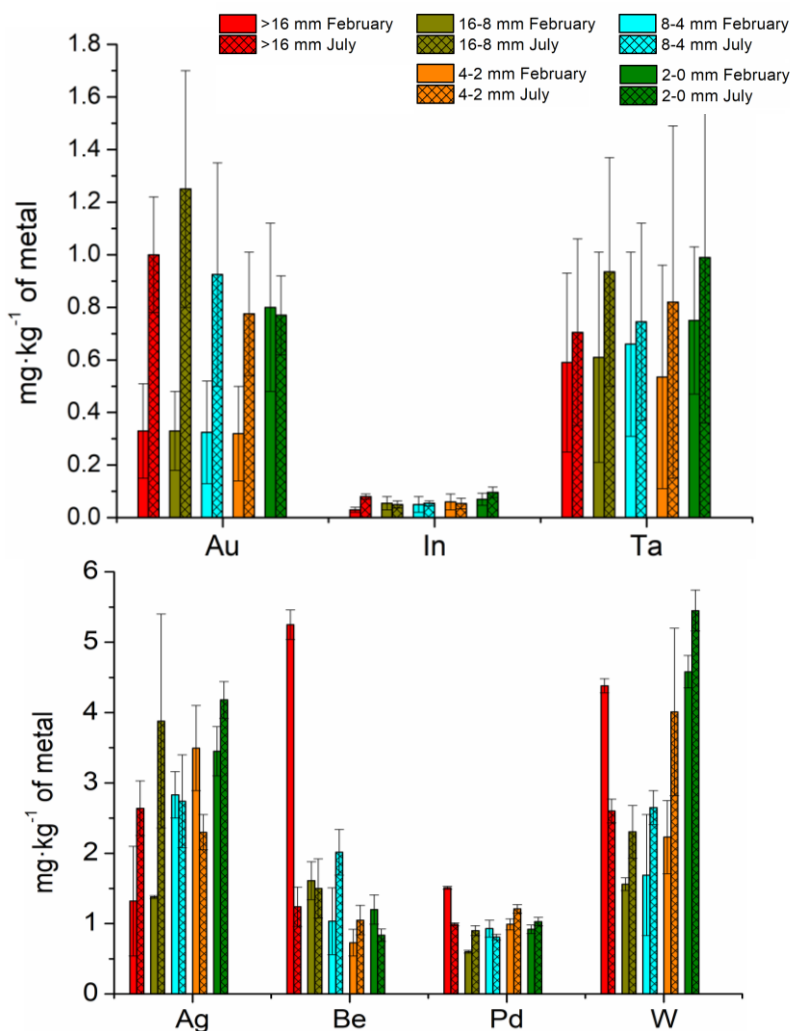


**Figure 15b.** Graphical comparison between the metal content in each particle size fraction for February WBA and July WBA, determined by total acid digestion.

As presented in *Figures 15a* and *15b*, almost for all metals and all particle sizes, the content of the metals studied is higher in July WBA than in February WBA. This fact might indicate that, during the summer, non-recycled WEED and other metallic trash increase considerably. A probable explanation for this is the incoming of tourism to the Catalan coast towns, since the incineration plant where WBA was collected is situated in an important touristic coast area (Tarragona and surroundings).

Furthermore, there are some cases where the metal content in a particular fraction is unexpectedly high (such as cobalt content in 8-4 mm fraction from July), which can be explained by the heterogeneous nature of the sample, especially in the metal part of each fraction. Heterogeneity of the metal samples can also explain some errors bars unusually high presented for few cases (error bars are calculated using the standard deviation of the pair of replicates of each subsample).

Clearly, the main metals in WBA are copper, aluminium, and magnesium, but also nickel is in considerable concentrations. These metals are considered base metals and they might come from a large range of objects, from simple machines to cutlery.

Antimony, lithium, cobalt, and gallium have quite high concentrations, as well. The amount of lithium detected might come mainly from batteries, ceramics, and glass; antimony is used for alloys, semiconductors and in TV screens, as well as a flame retardant for many articles; cobalt is found in ion-Li batteries, in alloys and as a catalyst; gallium is used mainly in semiconductors.

Silver, beryllium, palladium, and tungsten have been found in concentrations between 1-10 mg·kg<sup>-1</sup>. Tungsten mainly comes from incandescent light bulbs, tungsten carbide in tools, W-alloyed steel, and even from the balls from ballpoint pens [14]. Silver, palladium, and beryllium are all widely used in EED. They can be found in cable and high-definition televisions, electrical contacts, connectors, and screens in cell phones and computers, as examples.

The lowest concentrated metals found have been gold, indium, and thallium, whereas iridium, platinum, and germanium have been analysed but their values were below the detection limit in ICP-MS (Ir detection limit: 0.025 mg·kg<sup>-1</sup>; Pt detection limit: 0.50 mg·kg<sup>-1</sup>; Ge detection limit: 0.50 mg·kg<sup>-1</sup>). Indium is used in semiconductors and for flat-TV and computer screens, gold is present in most of connectors in EED and thallium is found in semiconductors and crystals for infrared instruments.

Additionally, a comparison between the sum of the metal content in each fraction (previously multiplied by their corresponding PSD percentage, as shown in *Figure 14*) and the metals concentration in Entire sample is useful to determine which process is the most efficient to extract a higher metal content of the sample, either applying the total acid digestion to the Entire sample or dividing WBA into different particle fractions. The following graphs (*Figure 16*) show

the comparison mentioned for February and July WBA, and related data is attached in *Table A.7* of Appendix 5.

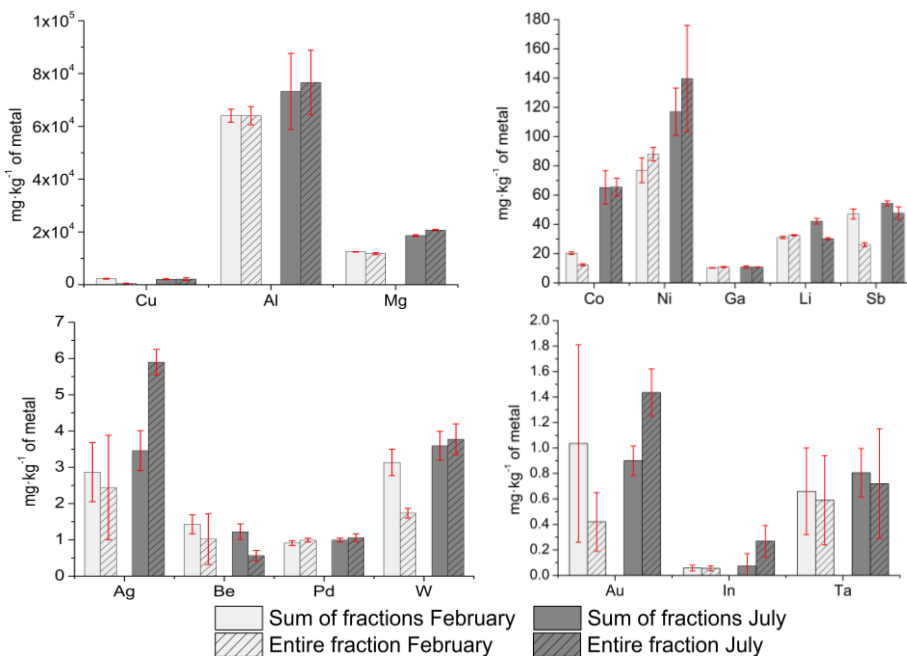


**Figure 16.** Graphical comparison between the sum of the metal content in each particle size fraction and the total content in the Entire sample of July WBA, determined by total acid digestion.

There is not a clear tendency in the graphics showed above in *Figure 16*, since it appears that in February WBA the most efficient way is to carry out the acid digestion previously separating the sample into five particle size fractions, whereas in most metals of July WBA the concentration founded in the Entire sample is higher than the sum of the particle size fractions results. Consequently, further studies should be performed to clarify this aspect.

Although the concentrations of critical metals found are relatively small if thinking about valorisation, it must be considered that the production of WBA in VECSA's valorisation plant is about 2,400,000 kg/month, which leads to an approximate amount of 2,016,000 kg/year of aluminium, 86 kg/year of silver and 29 kg/year of gold, as examples. These quantities are bigger enough to consider WBA as an important source of raw materials.

6.6.2. Sequential Extraction

Results obtained from sequential extraction procedure allow determining the mobility for every metal analysed in each extraction environment, which is related to the metal chemical speciation. Data obtained for July WBA is presented in *Tables A.8. to A.22.* of Appendix 6, and plotted in *Figures 17a, b and c.* A comparison between the total amount of each metal extracted during the sequential extraction procedure and the value obtained for the total acid digestion is performed and shown in *Figures 17 a, b, and c,* as well. Its aim is to evaluate the effectiveness of the sequential extraction method used in front of the total acid digestion.

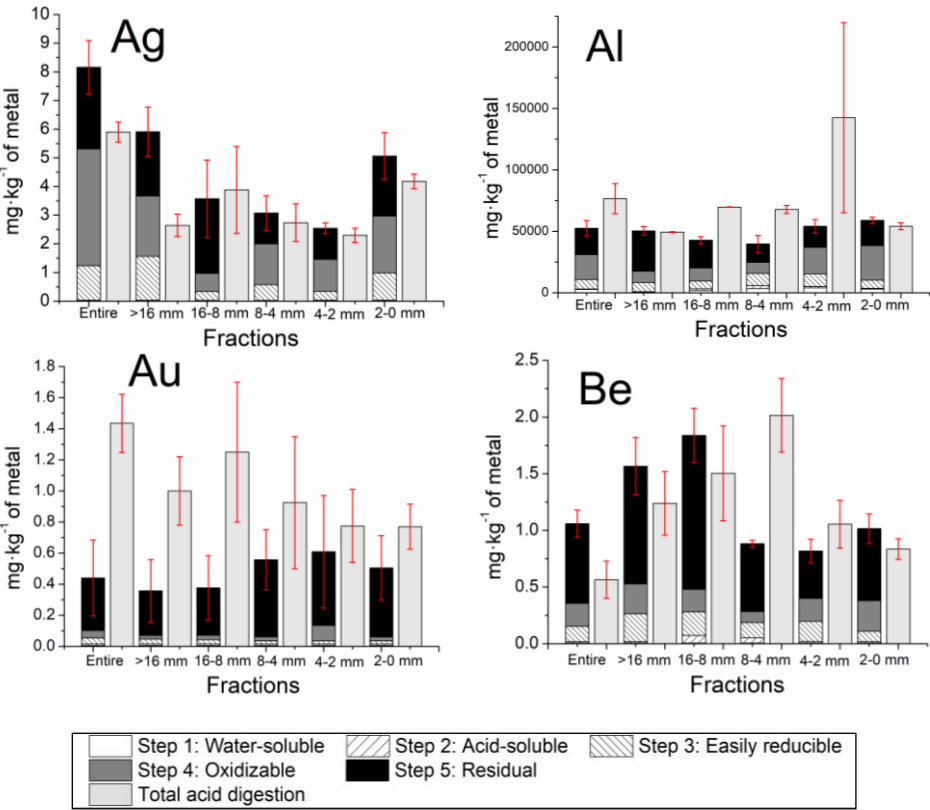


**Figure 17a.** Results obtained for Ag, Al, Au, and Be, after analysing the leachates for a five-step sequential extraction procedure, and their comparison with the result of total acid digestion for Entire fraction.



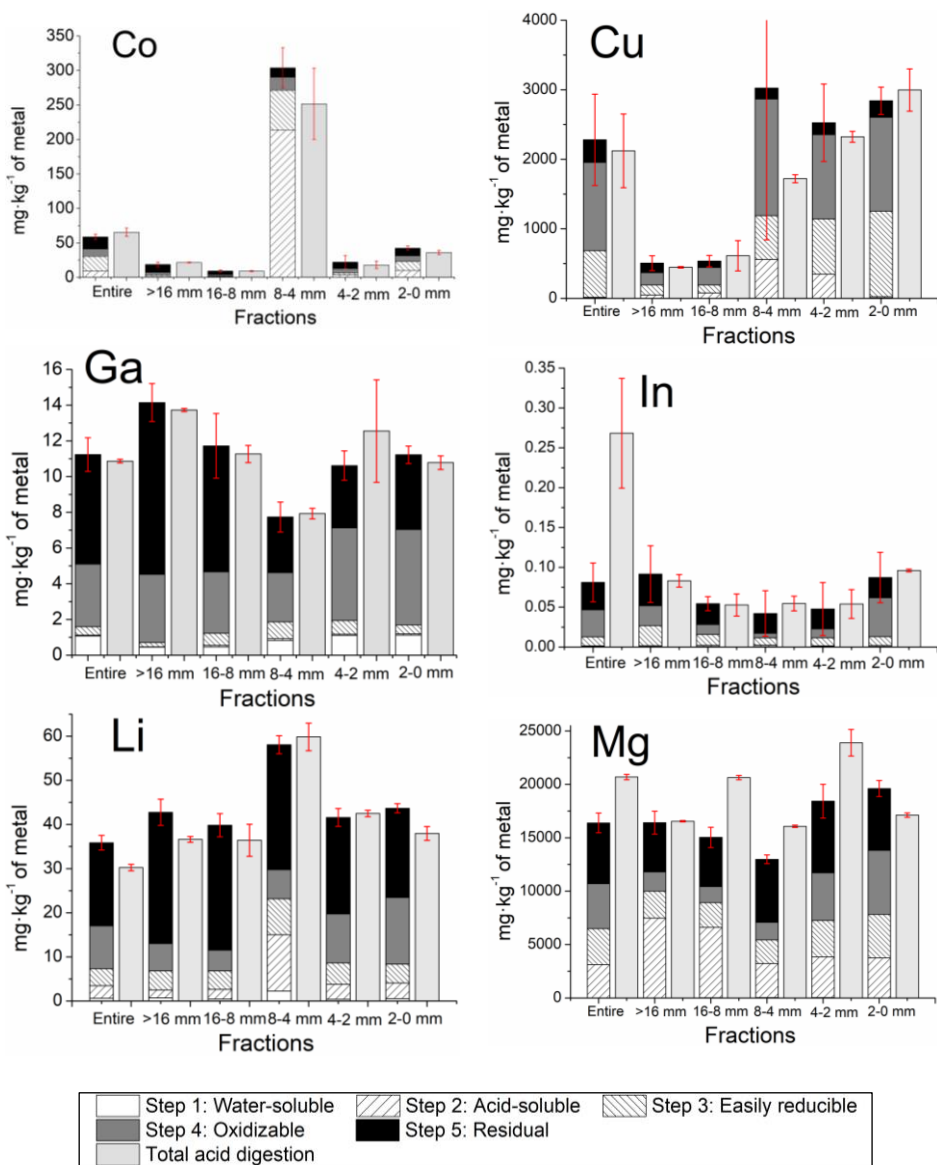


**Figure 17b.** Results obtained for Co, Cu, Ga, In, Li, and Mg, after analysing the leachates for a five-step sequential extraction procedure, and their comparison with the result of total acid digestion for Entire fraction.

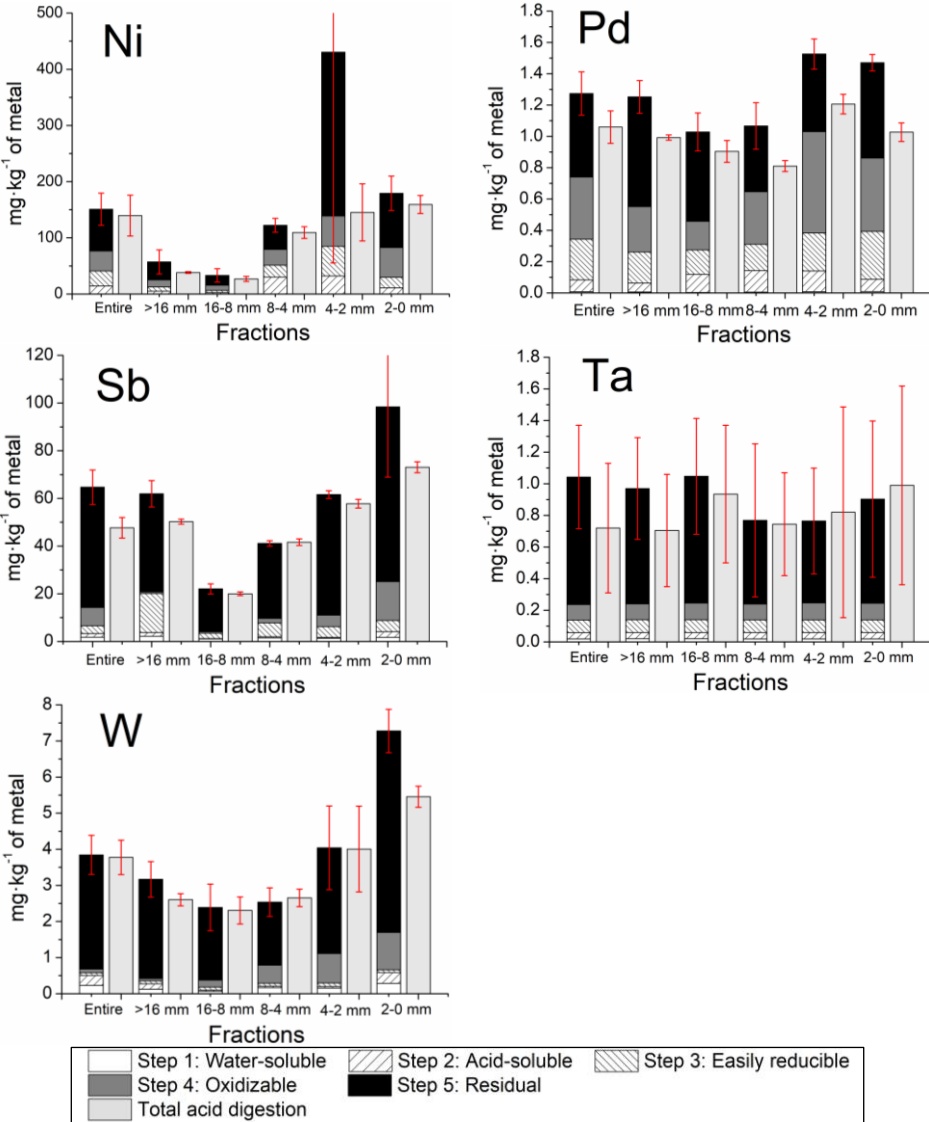


**Figure 17c.** Results obtained for Ni, Pd, Sb, Ta, and W, after analysing the leachates for a five-step sequential extraction procedure, and their comparison with the result of total acid digestion for Entire fraction.

Figures 17 a, b, and c show the amount of every metal extracted in each step of the sequential extraction for each particle size fraction, which is useful for the determination of the fraction

where the concentration of a particular metal is higher. The results are the mean of two replicates for each sample.

It is found that Au, Be, Li, Ni, Sb, Ta, and W are mainly released in step 5, which means that they are found mainly in their crystalline structure and they are well stabilised in the matrix on the material, thus a strong acid digestion is needed to extract them. For Ag, Al, Ga, In, and Pd, the content extracted in steps 4 and 5 are quite similar, thus these metals are both in their crystalline structure and bound to organic matter. In the case of Ga, it is also extracted during step 1 (water environment), therefore it is partly absorbed on the surface of solid particles and is easily released. Cu is mainly in its oxidized chemical form, as it is highly extracted in step 3. Co is mainly released during step 2, which means that it might be bound to carbonates and released in acid environment. Finally, Mg is obtained considerably in all steps except step 1, thus this metal is found in all chemical forms previously mentioned except in the absorbed form.

Data obtained shows that it would be difficult to easily valorise the metals contained in WBA, therefore an extreme acid or oxidizing environment will be needed to extract most of their content from the matrix.

Concerning the effectiveness of the sequential extraction method compared to the total acid digestion, the results from the sum of the five steps and those for the acid digestion are considerably similar, except for Au, Be, Pd, and Mg. In the case of Au, Be, and Pd, the little quantities found of those metals can increase the error found, while the differences in Mg can be associated to the heterogeneity of the sample. Considering that the possibility to commit experimental error in the sequential extraction procedure is higher than in the total acid digestion, the deviation of the results is acceptable and, in many cases, similar to the experimental error of the acid digestion. Only in some cases, experimental error is unusually big, again associated to the heterogeneity of the sample, especially in the metal subsamples.

Aluminium and magnesium are the unique metals whose results for the sequential extraction procedure and the total acid digestion can be compared to the XRF ones obtained (section 6.5.). For both elements, the order of magnitude of the results obtained for the three methods is the same. The distribution of the elements along the five particle sizes is similar for XRF and sequential extraction results, whereas for the total acid digestion is not clear enough.

6.6.3. X-Ray Diffraction

Although the initial sample of WBA has shown to be quite amorphous (an irregular, noisy and high baseline is registered), some mineralogical phases have been detected. Clearly, the main crystalline phases are calcite ( $\text{CaCO}_3$ ) and quartz ( $\text{SiO}_2$ ), but it is also possible to distinguish hydroxylapatite ( $\text{Ca}_5(\text{PO}_4)_3\text{Cl}_{0.5}(\text{OH})_{1.5}$ ), anhydrite ( $\text{CaSO}_4$ ), sodium calcium aluminium silicate ( $\text{NaCaAlSi}_2\text{O}_7$ ), potassium and calcium feldspars ( $\text{K}_x\text{Na}_{1-x}\text{Al}_y\text{Si}_{4-y}\text{O}_8$ ), calcium aluminium chloride hydroxide dihydrate ( $\text{Ca}_2\text{Al}(\text{OH})_6\text{Cl}\cdot 2\text{H}_2\text{O}$ ), gehlenite ( $\text{Ca}_2\text{Al}(\text{AlSiO}_7)$ ), calcium silicate ( $\text{Ca}_2(\text{SiO}_4)$ ), calcium silicate hydroxide ( $\text{Ca}_6\text{Si}_2\text{O}_7\text{SiO}_4(\text{OH})_2$ ), hydrocalumite ( $\text{Ca}_8\text{Al}(\text{OH})_6(\text{CO}_3)\text{Cl}_{1-x}(\text{OH})_x\cdot 3\text{H}_2\text{O}$ ), and orthoferrosilite ( $(\text{Fe}_{0.115}\text{Mg}_{0.885})(\text{Fe}_{0.383}\text{Mg}_{0.617})\text{Si}_2\text{O}_6$ ). However, the presence of all these crystalline phases is not confirmed due to the difficulty analysing the XRD diffractogram. Diffraction patterns found for WBA are attached in Appendix 7, Figure A.3. Besides, Table 2 is a summary of the results of XRD for the sequential extraction procedure residues and some explanations. Diffractograms for WBA and for each residue are presented in Figure A.4. of Appendix 7.

Table 2. Results from sequential extraction obtained by XRD analysis.

Initial compounds in WBA	After Step 1	After Step 2	After Step 3	After Step 4
Calcium Silicate Hydroxide	√	√	√	√*
Quartz	√	√	√	√
Gehlenite	√	√	x***	x
Hydroxylapatite	√	√	√	x
Hydrocalumine	x	x	x	x
Calcium Aluminum Chloride Hydroxide Hydrate	x	x	x	x
Calcite	√	√*	x***	x
Anhydrite	x	x	x	x
Sodium Calcium Aluminm Silicate	√	√	√	√*
Potassium-Feldspar	√	√	x***	x
Orthoferrosilite	√	√	x***	x
Calcium Silicate	√	√	x***	x
Calcium Acetate	--- **	√	x	x
Ammonium Nitrate	--- **	--- **	√	√
Ammonium Chloride	--- **	--- **	√	x
√ detected by XRD				
x not detected by XRD				
--- not present in the initial sample				
* decreasing of peaks intensity				
** coming from the extraction reagent used				
*** dissolved completely because of the pH of the reagent, not for the reducing environment [15]				

## 7. CONCLUSIONS

In this project, two different WBA samples from different seasons were evaluated. It is important to highlight that the great heterogeneity of WBA causes high error bars and big variation of results between the samples of WBA from the two months. Nevertheless, it can be extracted that the metals content studied for the WBA sample in July is higher than that from February.

The main metals obtained, determined by total acid digestion, for both WBA samples under study were Al, Mg, and Cu, but also Ni is in considerable concentrations. On the other hand, the minority metals founded in both WBA samples were Au, In, and Ta, while Ir, Pt, and Ge have been under the limit of detection of ICP-MS and ICP-OES. The sum of the results of all particle size fractions according to the PSD, have been compared to the result obtained for the Entire fraction of the February WBA and July WBA, giving ambiguous results. Therefore, further studies should be performed to clear up this question.

The sequential extraction performed shows that most of the metals analysed are mainly released during the steps 4 and 5 of the sequential extraction, and only few of them are extracted during steps 1-3. For this reason, the valorisation of the critical metals assessed in WBA is difficult as most of the metals analysed need an extreme acid or oxidizing environment to be extracted. XRD analysis for the initial sample and the residues of the sequential extraction steps show the mineralogical phases which disappear in each step, verifying the effect of the reagent used in each step.

The effectiveness of the sequential extraction procedure applied is considered acceptable, as the amount of metals extracted during the five-step procedure is comparable to the amount extracted in the total acid digestion. The only exceptions to this statement are Au, Be, Pd, and Mg, where the heterogeneity of the sample and the little quantities found of Au, Be, and Pd can

be an explanation for the differences founded. Furthermore, the experimental error committed during the sequential extraction is acceptable and comparable to the total acid digestion error.

Previous the WBA characterisation, a PSD assay has been performed obtaining a similar characteristic profile for both analysed samples, where the less representative particle size fraction is  $>16$  mm, and the most abundant fraction is 2-0 mm (over the 40% of mass of the total sample). IR spectroscopy has shown similar spectrum for all particle size fractions, as well as for WBA samples from both February and July. Peaks from the quartz typical vibrations, carbonates and silicates have been found, as well as those for hydration and interlayer water. XRF analysis has determined that the main elements are silicon, calcium, and aluminium, but also iron, magnesium, sodium, manganese, titanium and potassium are in considerable concentrations. Finally, it was also concluded that the particle size fractions which contain more metals are the smallest ones (2-0 mm and 4-2 mm).

To conclude, as the quantity of residues produced in Europe is growing, it is enormously important to found available procedures to recuperate the raw materials contained. The evaluation and extraction of critical metals in WBA samples from municipal waste incinerating plants are mandatory as their recyclability and reuse contribute to a circular economy and to the efficient use of resources.

## 8. REFERENCES AND NOTES

- [1] M. F. Ashby, "Materials and the Environment: Eco Informed Material Choice," *Mater. Today*, vol. 12, no. 5, p. 616, 2013.
- [2] COMMISSION OF THE EUROPEAN COMMUNITIES, "The raw materials initiative — meeting our critical needs for growth and jobs in Europe," p. 14, 2008.
- [3] Comisión Europea, "Lista de 2017 de materias primas fundamentales para la UE," p. 8, 2017.
- [4] K. Kahle *et al.*, "Bottom Ash from WTE Plants: Metal Recovery and Utilization," 2015.
- [5] European Commission, "Commission Decision on the European List of Waste (COM 2000/532/EC)," *Off. J. Eur. Communities*, vol. 2000D0532, no. 01.01.2002, pp. 1–31, 2000.
- [6] G. Wielgosiński, D. Wasiak, and A. Zawadzka, "The Use of Sequential Extraction for Assessing Environmental Risks of Waste Incineration Bottom Ash/Wykorzystanie Ekstrakcji Sekwencyjnej Do Oceny Zagrożeń Dla Środowiska Powodowanych Przez Żużle I Popioły Z," *Ecol. Chem. Eng. S*, vol. 21, no. 3, pp. 413–423, 2014.
- [7] G. de Catalunya and D. de M. Ambient, "Ordre de 15 de febrer de 1996, sobre valorització d'escories," *Dogc 2181- 13.03.1996*. pp. 1–8, 1996.
- [8] D. R. Lide, *CRC Handbook of Chemistry and Physics*. Advisory Board, 2005.
- [9] VECSA, "Proceso de valorización de las escorias de incineración," p. 4.
- [10] J. Chimenos, M. Segarra, M. . Fernández, and F. Espiell, "Characterization of the bottom ash in municipal solid waste incinerator," *J. Hazard. Mater.*, vol. 64, no. 3, pp. 211–222, 1999.
- [11] BERGHOF, "Theory of Sample Preparation Using Acid Digestion , Pressure Digestion and Microwave Digestion ( Microwave Decomposition )." Eningen, p. 11.
- [12] A. G. Norman and P. F. Pratt, "Digestion with hydrofluoric and perchloric acids for total," in *Methods of Soil Analysis*, Riverside, California: American Society of Agronomy, Soil Science Society of America, 1965.
- [13] A. Tessier, P. G. C. Campbell, and M. Bisson, "Sequential Extraction Procedure for the Speciation of Particulate Trace Metals," *Anal. Chem.*, vol. 51, no. 7, pp. 844–851, 1979.
- [14] L. S. Morf *et al.*, "Precious metals and rare earth elements in municipal solid waste - Sources and fate in a Swiss incineration plant," *Waste Manag.*, vol. 33, no. 3, pp. 634–644, 2013.
- [15] M. Draft--, "Waste and Biomass Valorization Multi-analytical approach and geochemical modeling for mineral trace element."
- [16] G. Rauret *et al.*, "Improvement of the BCR three step sequential extraction procedure prior to the certification of new sediment and soil reference materials," *J. Environ. Monit.*, vol. 1, no. 1, pp. 57–61, 1999.
- [17] G. Zhen *et al.*, "Characterization of controlled low-strength material obtained from dewatered sludge and refuse incineration bottom ash: Mechanical and microstructural perspectives," *J. Environ. Manage.*, vol. 129, pp. 183–189, 2013.
- [18] L.-G. Hwa, S.-L. Hwang, and L.-C. Liu, "Infrared and Raman spectra of calcium alumino-silicate glasses," *J. Non. Cryst. Solids*, vol. 238, no. 3, pp. 193–197, 1998.

## 9. ACRONYMS

<b>AAS</b>	Atomic Absorption Spectroscopy
<b>AFS</b>	Atomic Fluorescence Spectroscopy
<b>BA</b>	Bottom Ash
<b>BCR</b>	Community Bureau of Reference
<b>CCiTUB</b>	Centres Científics i Tecnològics de la Universitat de Barcelona
<b>CSIC</b>	Consejo Superior de Investigaciones Científicas
<b>DIOPMA</b>	Disseny i Optimització de Processos i Materials
<b>EED</b>	Electric and Electronic Devices
<b>HDPE</b>	High-Density Polyethylene
<b>ICP-MS</b>	Induction Coupled Plasma-Mass Spectrometry
<b>ICP-OES</b>	Induction Coupled Plasma-Optical Emission Spectrometry
<b>IDAEA</b>	Institut de Diagnosi Ambiental i Estudis de l'Aigua
<b>MW</b>	Municipal Waste
<b>PSD</b>	Particle-Size Distribution
<b>SIRUSA</b>	Servei d'Incineració dels Residus Urbans S.A.
<b>VECSA</b>	Valorización de Escorias de la Combustión, SA
<b>WBA</b>	Weathered Bottom Ash
<b>WEED</b>	Waste of Electric and Electronic Devices
<b>XRD</b>	X-Ray Diffraction
<b>XRF</b>	X-Ray Fluorescence



# APPENDICES



# APPENDIX 1: PARTICLE SIZE DISTRIBUTION DATA

Table A.1. Data for PSD of WBA from February and July.

Fracction	FEBRUARY		JULY	
	Mass for each fraction (g)	Percentage (%)	Mass for each fraction (g)	Percentage (%)
>16 mm	1992	5.96	1266	7.18
16-8 mm	5591	16.73	3003	17.03
8-4 mm	6334	18.96	3090	17.53
4-2 mm	5311	15.90	2871	16.29
2-0 mm	14184	42.45	7400	41.98
SUM	33412	100.00	17630	100.00

# APPENDIX 2: METALS REMOVAL DATA

Table A.2. Data for metal and non-metal parts of WBA from February and July.

Fracction	FEBRUARY		JULY	
	Non-metal (%)	Metal (%)	Non-metal (%)	Metal (%)
Entire	98.71	1.29	88.80	11.20
>16 mm	99.81	0.19	97.11	2.89
16-8 mm	95.07	4.93	83.53	16.47
8-4 mm	94.10	5.90	87.34	12.66
4-2 mm	95.19	4.81	82.47	17.53
2-0 mm	94.24	5.76	89.45	10.55

## APPENDIX 3: IR SPECTRA FOR WBA

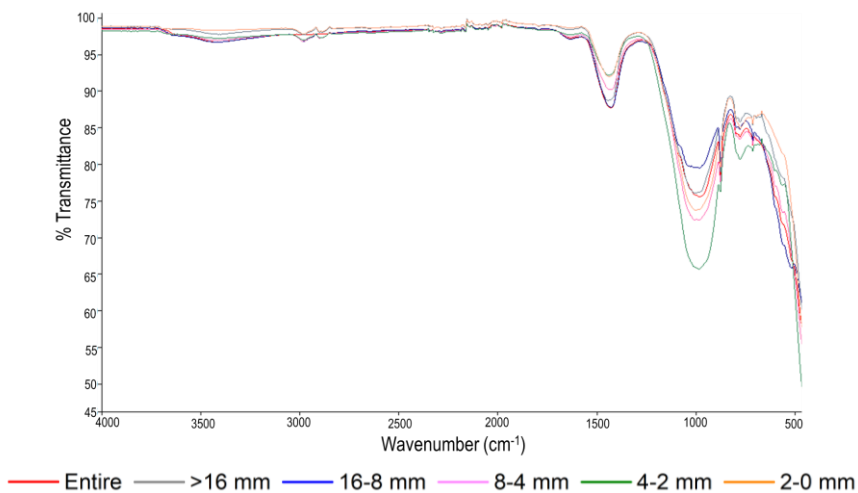


**Figure A.1.** IR spectra for all fractions of July WBA (particle size fractions and entire).

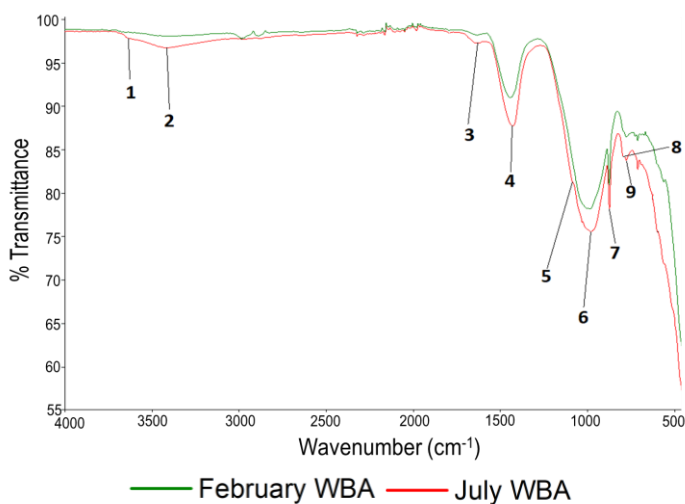


**Figure A.2.** Comparison between February and July WBA IR spectra. The peaks numbered are assigned in *Table 1* (section 6.4).

## APPENDIX 4: XRF RESULTS FOR WBA

**Table A.3.** XRF results for WBA from February and July.

FEBRUARY (fused disks)							JULY (pelletizing)					
%	Entire	>16 mm	16-8 mm	8-4 mm	2-4 mm	0-2 mm	Entire	>16 mm	16-8 mm	8-4 mm	2-4 mm	0-2 mm
Fe <sub>2</sub> O <sub>3</sub>	3.78	2.14	6.41	3.81	5.53	6.99	3.81	3.2	3.46	3.63	3.97	3.19
MnO	0.075	0.039	0.068	0.057	0.092	0.114	-	-	-	-	-	-
TiO <sub>2</sub>	0.39	0.49	0.26	0.33	0.52	0.78	0.83	0.67	0.47	0.65	0.85	1.07
CaO	15.19	9.77	13.42	15.27	17.18	23.07	25.9	19.9	17.1	18.4	24.8	28.8
K <sub>2</sub> O	1.36	1.77	1.13	1.19	1.30	1.05	1.55	2.15	1.67	1.31	1.82	1.58
P <sub>2</sub> O <sub>5</sub>	0.84	0.43	0.30	0.68	1.39	1.95	1.48	0.29	0.56	1.09	1.81	2.09
SiO <sub>2</sub>	53.42	61.56	59.49	56.88	46.26	27.54	30.6	40.6	48.5	50.6	41.2	23.1
Al <sub>2</sub> O <sub>3</sub>	9.89	11.43	4.99	5.62	9.75	12.33	6.25	6.43	5.87	5.34	6.71	6.94
MgO	2.17	1.46	1.97	1.74	2.64	2.64	2.57	2.48	2.05	1.41	3.05	2.86
Na <sub>2</sub> O	7.58	4.82	9.02	9.15	6.71	3.18	1.65	2.05	3.45	3.76	2.79	1.53
SO <sub>3</sub>	-	-	-	-	-	-	2.11	1.91	0.52	0.89	1.51	2.97

**Table A.4.** XRF results for the residues of the Entire sample of July WBA after each step of the sequential extraction procedure. Preparation of sample: pelletizing (Entire sample), loose powders (residues).

%	Initial July WBA	After Step 1	After Step 2	After Step 3	After Step 4
MgO	2.57	2.14±0.06	2.51±0.01	1.42±0.08	0.89±0.24
Al <sub>2</sub> O <sub>3</sub>	6.25	4.43±0.17	7.21±0.37	4.45±0.42	4.28±0.07
SiO <sub>2</sub>	30.6	31.4±0.4	44.90±0.7	43.2±0.6	38.8±0.2
P <sub>2</sub> O <sub>5</sub>	1.48	1.74±0.01	2.51±0.22	2.55±0.04	0.88±0.01
SO <sub>3</sub>	2.11	1.86±0.05	0.57±0.03	0.27±0.02	0.10±0.05
K <sub>2</sub> O	1.55	1.77±0.06	2.42±0.41	1.91±0.01	1.46±0.16
CaO	25.9	35.1±0.0	24.75±0.5	14.2±0.1	5.9±0.3
TiO <sub>2</sub>	0.83	1.47±0.01	1.95±0.13	2.28±0.00	1.94±0.03
Fe <sub>2</sub> O <sub>3</sub>	3.81	5.54±0.02	7.81±0.06	7.75±0.20	6.97±0.12

## APPENDIX 5: TOTAL ACID DIGESTION RESULTS

**Table A.5.** Total acid digestion data for February WBA. Results are shown for the 6 particle size fractions.

mg·kg <sup>-1</sup>	Co ± σ	Ni ± σ	Ag ± σ	Au ± σ	Be ± σ
>16 mm	11.5±0.0	26.5±0.5	1.32±0.78	0.325±0.181	5.25±0.21
16-8 mm	8.81±0.25	62.2±6.7	1.38±0.02	0.330±0.154	1.61±0.27
8-4 mm	9.81±0.65	38.1±6.0	2.83±0.33	0.325±0.202	1.04±0.48
4-2 mm	15.6±2.0	71.5±9.1	3.50±0.61	0.320±0.180	0.730±0.193
2-0 mm	32.7±0.9	109±11	3.45±0.35	0.803±0.319	1.20±0.21
Entire	12.4±0.7	88.0±4.6	2.44±1.44	0.420±0.231	1.02±0.23

mg·kg <sup>-1</sup>	Ga ± σ	In ± σ	Li ± σ	Pd ± σ	Sb ± σ
>16 mm	15.4±0.0	0.030±0.007	34.8±0.2	1.51±0.02	18.5±0.3
16-8 mm	8.07±0.35	0.055±0.025	29.2±0.4	0.595±0.022	46.6±1.6
8-4 mm	7.84±0.37	0.050±0.032	33.7±1.0	0.927±0.118	64.9±4.2
4-2 mm	11.8±0.2	0.055±0.030	39.6±1.4	0.985±0.076	41.2±2.8
2-0 mm	10.9±0.1	0.065±0.023	26.9±0.6	0.917±0.062	45.6±4.3
Entire	10.8±0.3	0.055±0.019	32.6±0.4	0.991±0.053	26.1±1.3

mg·kg <sup>-1</sup>	Ta ± σ	W ± σ	Cu ± σ	Al ± σ	Mg ± σ
>16 mm	0.590±0.344	4.38±0.10	81.1±1.2	56682±752	7445±47
16-8 mm	0.610±0.402	1.56±0.09	2837±222	58789±4804	11128±172
8-4 mm	0.660±0.350	1.69±0.86	1359±55	62562±3164	9856±46
4-2 mm	0.535±0.434	2.23±0.52	4092±512	89414±4989	14757±149
2-0 mm	0.750±0.283	4.58±0.23	2074±59	58301±559	14043±105
Entire	0.590±0.361	1.73±0.14	498±86	64038±3465	11769±379

Table A.6. Total acid digestion data for July WBA. Results are shown for the 6 particle size fractions.

mg·kg <sup>-1</sup>	Co ± σ	Ni ± σ	Ag ± σ	Au ± σ	Be ± σ
>16 mm	21.5±0.6	38.2±1.5	2.64±0.39	1.00±0.22	1.24±0.28
16-8 mm	9.04±0.67	26.9±4.6	3.88±1.52	1.25±0.45	1.50±0.42
8-4 mm	252±52	109±10	2.74±0.66	0.925±0.434	2.02±0.33
4-2 mm	18.0±5.4	145±51	2.30±0.25	0.775±0.242	1.05±0.21
2-0 mm	36.1±3.1	159±16	4.18±0.26	0.770±0.152	0.835±0.103
Entire	65.5±6.1	140±36	5.90±0.35	1.44±0.19	0.565±0.170

mg·kg <sup>-1</sup>	Ga ± σ	In ± σ	Li ± σ	Pd ± σ	Sb ± σ
>16 mm	13.7±0.1	0.083±0.008	36.6±0.7	0.992±0.021	50.3±1.0
16-8 mm	11.3±0.5	0.053±0.014	36.4±3.6	0.904±0.073	20.0±0.8
8-4 mm	7.93±0.30	0.055±0.010	59.9±3.1	0.811±0.043	41.6±1.4
4-2 mm	12.6±2.9	0.054±0.020	42.5±0.7	1.21±0.06	57.8±1.8
2-0 mm	10.8±0.4	0.096±0.021	38.0±1.6	1.03±0.06	73.1±2.3
Entire	10.9±0.1	0.268±0.123	30.2±0.7	1.06±0.10	47.7±4.3

mg·kg <sup>-1</sup>	Ta ± σ	W ± σ	Cu ± σ	Al ± σ	Mg ± σ
>16 mm	0.705±0.361	2.60±0.17	446±11	49340±363	16546±65
16-8 mm	0.935±0.442	2.31±0.38	612±219	69717±216	20640±201
8-4 mm	0.745±0.381	2.65±0.24	1721±57	67798±3272	16072±108
4-2 mm	0.820±0.674	4.01±1.19	2323±79	142470±77325	23901±1249
2-0 mm	0.990±0.630	5.45±0.29	2996±304	54165±2791	17124±202
Entire	0.720±0.431	3.78±0.43	2122±530	76605±12242	20689±247

Table A.7. Comparison between the sum of the metal content in each fraction and in the Entire sample.

FEBRUARY			JULY	
mg·kg <sup>-1</sup>	Sum of fractions	Entire fraction	Sum of fractions	Entire fraction
Co	20.4±0.9	12.4±0.7	65.3±11.4	65.5±6.1
Ni	77.0±8.4	88.0±4.6	117±16	140±36
Ag	2.87±0.82	2.44±1.44	3.46±0.55	5.90±0.35
Au	1.04±0.78	0.423±0.230	0.900±0.116	1.44±0.19
Be	1.43±0.26	1.02±0.71	1.23±0.22	0.565±0.145
Ga	10.3±0.2	10.8±0.3	10.9±0.8	10.9±0.1
In	0.057±0.023	0.055±0.019	0.073±0.097	0.268±0.123
Li	31.1±0.8	32.5±0.4	42.2±2.0	30.2±0.7
Pd	0.911±0.066	0.991±0.053	0.995±0.054	1.06±0.10
Sb	47.1±3.4	26.1±1.3	54.4±1.7	47.7±4.3
Ta	0.661±0.342	0.590±0.352	0.805±0.191	0.720±0.430
W	3.14±0.37	1.73±0.14	3.59±0.40	3.78±0.43
Cu	2268±154	498±86	2074±189	2122±530
Al	64041±2479	64038±3465	73238±14401	76605±12242
Mg	12482±109	11769±379	18601±346	20689±247

## APPENDIX 6: SEQUENTIAL EXTRACTION DATA

**Table A.8.** Sequential extraction data for **cobalt**. Results are shown for the 6 particle size fractions.

mg·kg <sup>-1</sup>	Entire ± σ	>16 mm ± σ	16-8 mm ± σ	8-4 mm ± σ	4-2 mm ± σ	2-0 mm ± σ
Step 1	0.012±0.002	0.006±0.008	0.008±0.010	0.004±0.007	0.008±0.009	0.008±0.010
Step 2	9.21±0.46	1.62±0.28	1.01±0.13	213 ±18	3.39±0.31	10.0±1.1
Step 3	21.4±1.0	2.41±0.09	0.869±0.067	57.8±6.2	3.19±0.27	13.0±0.8
Step 4	10.6±0.3	3.17±0.66	2.00±0.56	18.8±1.9	6.05±3.69	8.18±0.40
Step 5	17.5±2.1	11.4±2.4	5.44±0.64	13.4±2.9	9.51±5.18	11.1±0.7
SUM	58.7±3.9	18.6±3.4	9.32±1.41	304±29	22.1±9.5	42.4±3.0
Total acid digestion	65.5±6.1	21.5±0.6	9.04±0.67	252±52	18.0±5.4	36.0±3.1

**Table A.9.** Sequential extraction data for **nickel**. Results are shown for the 6 particle size fractions.

mg·kg <sup>-1</sup>	Entire ± σ	>16 mm ± σ	16-8 mm ± σ	8-4 mm ± σ	4-2 mm ± σ	2-0 mm ± σ
Step 1	0.153±0.196	0.130±0.154	0.079±0.087	0.102±0.122	0.151±0.171	0.173±0.243
Step 2	14.2±5.4	4.74±3.39	2.41±2.71	30.1±7.0	32.2±22.5	11.1±2.9
Step 3	26.5±6.0	7.67±0.49	3.97±0.73	21.1±0.7	52.7±7.7	18.5±7.5
Step 4	35.6±4.3	12.7±1.7	9.15±1.62	28.1±1.6	53.7±15.1	53.0±1.2
Step 5	74.4±12.7	31.9±15.8	17.5±6.9	42.9±2.9	292±330	96.4±18.8
SUM	150±28	57.1±21.5	33.1±12.0	122±12	430±375	179±31
Total acid digestion	139±36	38.2±1.5	26.845±4.565	109±10	145±51	159±16

**Table A.10.** Sequential extraction data for **silver**. Results are shown for the 6 particle size fractions.

mg·kg <sup>-1</sup>	Entire ± σ	>16 mm ± σ	16-8 mm ± σ	8-4 mm ± σ	4-2 mm ± σ	2-0 mm ± σ
Step 1	0.010±0.010	0.010±0.011	0.009±0.009	0.010±0.010	0.010±0.010	0.010±0.010
Step 2	0.020±0.020	0.020±0.021	0.020±0.020	0.016±0.028	0.020±0.018	0.023±0.018
Step 3	1.21±0.21	1.53±0.04	0.308±0.019	0.550±0.115	0.312±0.021	0.954±0.204
Step 4	4.07±0.35	2.11±0.11	0.634±0.113	1.42±0.14	1.12±0.02	1.98±0.28
Step 5	2.85±0.34	2.24±0.68	2.60±1.19	1.08±0.31	1.08±0.12	2.09±0.31
SUM	8.16±0.93	5.91±0.86	3.57±1.35	3.07±0.61	2.54±0.19	5.06±0.82
Total acid digestion	5.90±0.35	2.64±0.39	3.88±1.52	2.74±0.66	2.30±0.25	4.18±0.26

**Table A.11.** Sequential extraction data for **gold**. Results are shown for the 6 particle size fractions.

mg·kg <sup>-1</sup>	Entire ± σ	>16 mm ± σ	16-8 mm ± σ	8-4 mm ± σ	4-2 mm ± σ	2-0 mm ± σ
Step 1	0.005±0.005	0.005±0.005	0.005±0.005	0.005±0.005	0.005±0.005	0.005±0.005
Step 2	0.010±0.010	0.010±0.011	0.010±0.010	0.010±0.011	0.010±0.010	0.010±0.010
Step 3	0.039±0.022	0.031±0.010	0.029±0.014	0.020±0.020	0.020±0.020	0.020±0.020
Step 4	0.047±0.003	0.025±0.026	0.028±0.023	0.027±0.024	0.100±0.096	0.026±0.022
Step 5	0.338±0.204	0.286±0.149	0.3055±0.155	0.496±0.133	0.474±0.230	0.444±0.149
SUM	0.440±0.244	0.357±0.202	0.376±0.207	0.557±0.193	0.609±0.361	0.505±0.207
Total acid digestion	1.44±0.19	1.00±0.22	1.25±0.45	0.925±0.425	0.775±0.235	0.770±0.145

**Table A.12.** Sequential extraction data for **beryllium**. Results are shown for the 6 particle size fractions.

mg·kg <sup>-1</sup>	Entire ± σ	>16 mm ± σ	16-8 mm ± σ	8-4 mm ± σ	4-2 mm ± σ	2-0 mm ± σ
Step 1	0.005±0.005	0.005±0.005	0.005±0.005	0.005±0.005	0.005±0.005	0.005±0.005
Step 2	0.012±0.011	0.013±0.012	0.068±0.003	0.048±0.004	0.015±0.010	0.013±0.010
Step 3	0.135±0.014	0.246±0.023	0.207±0.033	0.134±0.005	0.178±0.010	0.091±0.005
Step 4	0.204±0.006	0.264±0.048	0.199±0.028	0.097±0.002	0.202±0.042	0.271±0.018
Step 5	0.703±0.083	1.04±0.17	1.36±0.17	0.600±0.014	0.418±0.038	0.635±0.091
SUM	1.06±0.119	1.57±0.25	1.84±0.24	0.882±0.031	0.818±0.104	1.02±0.13
Total acid digestion	0.565±0.165	1.24±0.28	1.50±0.42	2.02±0.33	1.05±0.21	0.835±0.091

**Table A.13.** Sequential extraction data for **gallium**. Results are shown for the 6 particle size fractions.

mg·kg <sup>-1</sup>	Entire ± σ	>16 mm ± σ	16-8 mm ± σ	8-4 mm ± σ	4-2 mm ± σ	2-0 mm ± σ
Step 1	1.08±0.04	0.445±0.018	0.469±0.010	0.827±0.046	1.11±0.03	1.12±0.07
Step 2	0.048±0.005	0.020±0.012	0.077±0.002	0.108±0.001	0.064±0.028	0.073±0.003
Step 3	0.468±0.108	0.242±0.039	0.683±0.080	0.931±0.202	0.762±0.102	0.496±0.046
Step 4	3.51±0.23	3.81±0.23	3.44±0.89	2.75±0.22	5.19±0.33	5.35±0.07
Step 5	6.13±0.56	9.62±0.77	7.05±0.83	3.12±0.37	3.49±0.32	4.18±0.30
SUM	11.2±0.9	14.1±1.1	11.7±1.8	7.74±0.84	10.6±0.8	11.2±0.5
Total acid digestion	10.9±0.1	13.7±0.1	11.3±0.5	7.93±0.30	12.5±2.9	10.8±0.4

**Table A.14.** Sequential extraction data for **indium**. Results are shown for the 6 particle size fractions.

mg·kg <sup>-1</sup>	Entire ± σ	>16 mm ± σ	16-8 mm ± σ	8-4 mm ± σ	4-2 mm ± σ	2-0 mm ± σ
Step 1	0.001±0.001	0.001±0.001	0.001±0.001	0.001±0.001	0.001±0.001	0.001±0.001
Step 2	0.001±0.001	0.001±0.001	0.002±0.000	0.002±0.000	0.001±0.001	0.001±0.001
Step 3	0.011±0.002	0.025±0.003	0.014±0.001	0.009±0.000	0.010±0.002	0.011±0.002
Step 4	0.034±0.000	0.025±0.006	0.013±0.002	0.006±0.002	0.011±0.004	0.049±0.003
Step 5	0.034±0.020	0.040±0.025	0.026±0.006	0.025±0.026	0.025±0.026	0.025±0.025
SUM	0.081±0.024	0.091±0.036	0.054±0.009	0.042±0.029	0.048±0.033	0.087±0.032
Total acid digestion	0.268±0.069	0.083±0.008	0.053±0.014	0.055±0.009	0.054±0.018	0.096±0.002

**Table A.15.** Sequential extraction data for **lithium**. Results are shown for the 6 particle size fractions.

mg·kg <sup>-1</sup>	Entire ± σ	>16 mm ± σ	16-8 mm ± σ	8-4 mm ± σ	4-2 mm ± σ	2-0 mm ± σ
Step 1	0.594±0.091	0.700±0.079	0.411±0.021	2.25±0.16	0.376±0.012	0.534±0.041
Step 2	2.86±0.12	1.83±0.07	2.20±0.05	12.8±0.1	3.40±0.14	3.56±0.00
Step 3	3.88±0.17	4.29±0.16	4.20±0.09	8.14±0.09	4.86±0.38	4.26±0.06
Step 4	9.67±0.02	6.20±0.88	4.71±0.95	6.61±0.38	11.1±0.8	15.1±0.1
Step 5	18.9±1.3	29.8±1.8	28.3±1.5	28.3±1.3	21.9±0.7	20.2±0.8
SUM	35.9±1.7	42.8±3.0	39.8±2.6	58.1±2.0	41.6±2.0	43.7±1.0
Total acid digestion	30.2±0.7	36.6±0.7	36.4±3.6	59.8±3.1	42.5±0.7	38.0±1.6

**Table A.16.** Sequential extraction data for **palladium**. Results are shown for the 6 particle size fractions.

mg·kg <sup>-1</sup>	Entire ± σ	>16 mm ± σ	16-8 mm ± σ	8-4 mm ± σ	4-2 mm ± σ	2-0 mm ± σ
Step 1	0.008±0.001	0.005±0.001	0.003±0.001	0.004±0.001	0.007±0.001	0.008±0.001
Step 2	0.076±0.004	0.058±0.001	0.116±0.005	0.138±0.005	0.132±0.007	0.078±0.002
Step 3	0.260±0.013	0.198±0.019	0.156±0.004	0.169±0.004	0.243±0.009	0.306±0.011
Step 4	0.397±0.078	0.290±0.024	0.182±0.038	0.335±0.129	0.647±0.044	0.469±0.015
Step 5	0.534±0.042	0.701±0.060	0.571±0.074	0.420±0.010	0.496±0.036	0.609±0.024
SUM	1.27±0.14	1.25±0.105	1.03±0.12	1.07±0.148	1.53±0.10	1.47±0.053
Total acid digestion	1.06±0.10	0.992±0.017	0.904±0.070	0.811±0.035	1.21±0.06	1.03±0.059



**Table A.17.** Sequential extraction data for **antimony**. Results are shown for the 6 particle size fractions.

mg·kg <sup>-1</sup>	Entire ± σ	>16 mm ± σ	16-8 mm ± σ	8-4 mm ± σ	4-2 mm ± σ	2-0 mm ± σ
Step 1	1.83±0.11	2.24±0.15	1.05±0.01	1.51±0.02	1.35±0.06	1.76±0.11
Step 2	1.42±0.56	1.54±0.54	0.13±0.01	0.442±0.252	0.363±0.119	2.36±1.01
Step 3	3.31±0.61	16.4±0.9	2.32±0.08	5.82±0.09	4.50±0.14	4.71±0.95
Step 4	7.68±2.32	0.69±0.03	0.62±0.45	1.93±0.39	4.79±0.66	16.3±2.5
Step 5	50.4±3.6	41.1±3.9	17.9±1.6	31.4±0.4	50.6±0.6	73.3±24.9
SUM	64.7±7.2	61.9±5.5	22.0±2.2	41.1±1.1	61.6±1.6	98.4±29.4
Total acid digestion	47.7±4.3	50.3±1.0	20.0±0.8	41.6±1.4	57.8±1.8	73.1±2.3

**Table A.18.** Sequential extraction data for **tantalum**. Results are shown for the 6 particle size fractions.

mg·kg <sup>-1</sup>	Entire ± σ	>16 mm ± σ	16-8 mm ± σ	8-4 mm ± σ	4-2 mm ± σ	2-0 mm ± σ
Step 1	0.020±0.000	0.020±0.001	0.020±0.000	0.020±0.000	0.020±0.000	0.020±0.000
Step 2	0.039±0.001	0.040±0.001	0.040±0.000	0.040±0.000	0.040±0.000	0.040±0.000
Step 3	0.079±0.001	0.080±0.002	0.080±0.000	0.080±0.000	0.080±0.000	0.080±0.000
Step 4	0.099±0.001	0.100±0.003	0.105±0.012	0.100±0.001	0.107±0.007	0.105±0.011
Step 5	0.806±0.324	0.730±0.315	0.802±0.353	0.529±0.482	0.518±0.328	0.658±0.483
SUM	1.04±0.33	0.970±0.321	1.05±0.366	0.769±0.484	0.765±0.334	0.903±0.494
Total acid digestion	0.720±0.410	0.705±0.355	0.935±0.435	0.745±0.325	0.820±0.666	0.990±0.629

**Table A.19.** Sequential extraction data for **tungsten**. Results are shown for the 6 particle size fractions.

mg·kg <sup>-1</sup>	Entire ± σ	>16 mm ± σ	16-8 mm ± σ	8-4 mm ± σ	4-2 mm ± σ	2-0 mm ± σ
Step 1	0.228±0.007	0.127±0.004	0.062±0.001	0.165±0.001	0.158±0.003	0.288±0.007
Step 2	0.277±0.014	0.148±0.012	0.041±0.000	0.047±0.002	0.040±0.005	0.301±0.023
Step 3	0.079±0.001	0.080±0.002	0.080±0.000	0.080±0.000	0.096±0.003	0.075±0.003
Step 4	0.097±0.001	0.067±0.024	0.195±0.072	0.496±0.108	0.820±0.176	1.03±0.32
Step 5	3.16±0.517	2.75±0.45	2.01±0.57	1.75±0.284	2.93±0.97	5.58±0.25
SUM	3.84±0.540	3.17±0.49	2.39±0.65	2.54±0.395	4.04±1.16	7.28±0.60
Total acid digestion	3.78±0.475	2.60±0.17	2.31±0.38	2.65±0.243	4.01±1.19	5.45±0.29

**Table A.20.** Sequential extraction data for **copper**. Results are shown for the 6 particle size fractions.

mg·kg <sup>-1</sup>	Entire ± σ	>16 mm ± σ	16-8 mm ± σ	8-4 mm ± σ	4-2 mm ± σ	2-0 mm ± σ
Step 1	4.70±0.18	1.31±0.04	1.54±0.11	1.64±0.15	2.32±0.83	6.25±0.34
Step 2	10.9±0.5	47.6±7.5	76.4±2.6	559±23	345±7	18.5±2.4
Step 3	670±21	144±19	114±3	628±50	796±55	1229±13
Step 4	1270±540	178±16	252±66	1678±1691	1212±450	1350±153
Step 5	325±96	135±63	91.9±10.5	157±418	171±45	237±27
SUM	2280±657	506±106	535±82	3023±2181	2525±557	2841±196
Total acid digestion	2122±530	446±11	612±219	1721±57	2323±79	2996±304

**Table A.21.** Sequential extraction data for **magnesium**. Results are shown for the 6 particle size fractions.

mg·kg <sup>-1</sup>	Entire ± σ	>16 mm ± σ	16-8 mm ± σ	8-4 mm ± σ	4-2 mm ± σ	2-0 mm ± σ
Step 1	5.01±5.40	6.09±5.96	22.9±6.7	33.3±2.1	36.0±0.6	14.6±0.5
Step 2	3132±88	7476±101	6580±146	3201±65	3810±51	3734±107
Step 3	3365±76	2523±39	2321±76	2196±24	3403±168	4075±26
Step 4	4195±461	1808±381	1508±424	1658±238	4477±690	5996±407
Step 5	5692±295	4606±547	4606±298	5895±83	6702±667	5790±210
SUM	16388±925	16418±1075	15038±950	12983±412	18427±1577	19610±750
Total acid digestion	20689±247	16546±65	20640±201	16072±108	23901±1249	17124±202

**Table A.22.** Sequential extraction data for **aluminium**. Results are shown for the 6 particle size fractions.

mg·kg <sup>-1</sup>	Entire ± σ	>16 mm ± σ	16-8 mm ± σ	8-4 mm ± σ	4-2 mm ± σ	2-0 mm ± σ
Step 1	2750±176	578±561	1798±38	3383±114	4049±306	3044±138
Step 2	434±95	212±113	1475±44	2350±45	1056±428	574±134
Step 3	7587±1170	7596±428	6319±56	10057±1048	10257±804	6698±319
Step 4	20240±2708	9195±1482	10608±1057	8873±1004	21571±2330	28083±1103
Step 5	21538±2087	32826±1432	22625±1706	15041±4604	17170±1636	20533±906
SUM	52548±6237	50407±3511	42825±2901	39705±6814	54104±5504	58932±2600
Total acid digestion	76605±12242	49340±363	69717±216	67798±3272	142470±77325	54165±2791

APPENDIX 7: XRD RESULTS FOR WBA AND FOR THE SEQUENTIAL EXTRACTION PROCEDURE

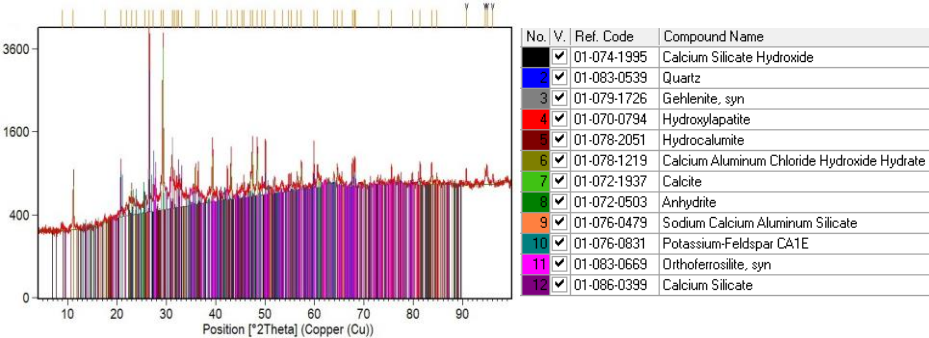


**Figure A.3.** X-Ray diffractogram for WBA with crystalline phases assigned. Each colour in the diffractogram is related with a reference compound pattern in the list on the right.

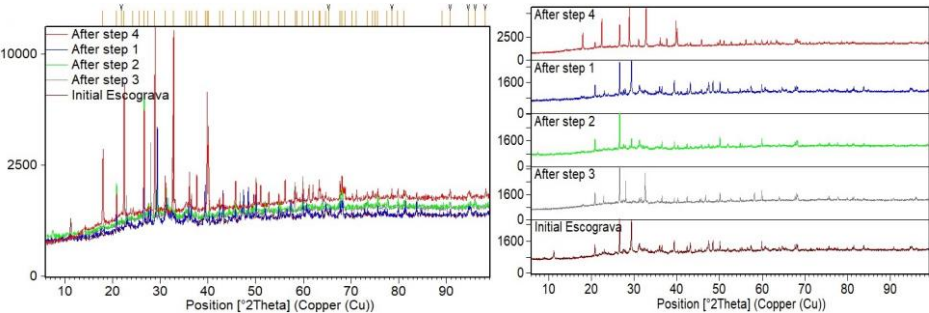


**Figure A.4.** X-Ray diffractograms for the five steps of the sequential extraction procedure. On the left, diffractograms are overlapped; on the right, diffractograms are shown separately to detect differences on peaks between them.







